



Inhibition of Renal Tubular Epithelial Mesenchymal Transition and Endoplasmic Reticulum Stress-Induced Apoptosis with Shenkang Injection Attenuates Diabetic Tubulopathy

OPEN ACCESS

Edited by:

Juei-Tang Cheng,
Chang Jung Christian University,
Taiwan

Reviewed by:

Baoqin Lin,
Guangzhou University of Chinese
Medicine, China
Shing-Hwa Liu,
National Taiwan University, Taiwan

*Correspondence:

Yi-Gang Wan
wyg68918@sina.com
Wei Wu
71340340@qq.com

[†]These authors have contributed
equally to this work and share first
authorship

[‡]These authors have contributed
equally to this work and share last
authorship

Specialty section:

This article was submitted to
Ethnopharmacology,
a section of the journal
Frontiers in Pharmacology

Received: 24 March 2021

Accepted: 21 July 2021

Published: 02 August 2021

Citation:

Wang W-W, Liu Y-L, Wang M-Z, Li H,
Liu B-H, Tu Y, Yuan C-C, Fang Q-J,
Chen J-X, Wang J, Fu Y, Wan Z-Y,
Wan Y-G and Wu W (2021) Inhibition of
Renal Tubular Epithelial Mesenchymal
Transition and Endoplasmic Reticulum
Stress-Induced Apoptosis with
Shenkang Injection Attenuates
Diabetic Tubulopathy.
Front. Pharmacol. 12:662706.
doi: 10.3389/fphar.2021.662706

Wen-Wen Wang^{1,2†}, Ying-Lu Liu^{3†}, Mei-Zi Wang^{1†}, Huan Li¹, Bu-Hui Liu⁴, Yue Tu⁵,
Can-Can Yuan¹, Qi-Jun Fang¹, Jia-Xin Chen¹, Jie Wang¹, Yan Fu¹, Zi-Yue Wan⁶,
Yi-Gang Wan^{3*‡} and Wei Wu^{3*‡}

¹Department of Traditional Chinese Medicine, Nanjing Drum Tower Hospital Clinical College of Nanjing University of Chinese Medicine, Nanjing, China, ²Department of Nephrology, Wenzhou Hospital of Integrated Traditional Chinese and Western Medicine, Wenzhou, China, ³Department of Traditional Chinese Medicine, Nanjing Drum Tower Hospital, The Affiliated Hospital of Nanjing University Medical School, Nanjing, China, ⁴Nephrology Division, Affiliated Hospital of Nanjing University of Chinese Medicine, Nanjing, China, ⁵Department of Traditional Chinese Medicine Health Preservation, Acupuncture, Moxibustion and Massage College, Health Preservation and Rehabilitation College, Nanjing University of Chinese Medicine, Nanjing, China, ⁶Graduate School of Social Sciences, Faculty of Social Sciences, Hitotsubashi University, Tokyo, Japan

Background: The proximal renal tubule plays a critical role in diabetic kidney disease (DKD) progression. Early glomerular disease in DKD triggers a cascade of injuries resulting in renal tubulointerstitial disease. These pathophysiological responses are collectively described as diabetic tubulopathy (DT). Thus, therapeutic strategies targeting DT hold significant promise for early DKD treatment. Shenkang injection (SKI) has been widely used to treat renal tubulointerstitial fibrosis in patients with chronic kidney disease in China. However, it is still unknown whether SKI can alleviate DT. We designed a series of experiments to investigate the beneficial effects of SKI in DT and the mechanisms that are responsible for its effect on epithelial-to-mesenchymal transition (EMT) and endoplasmic reticulum (ER) stress-induced apoptosis in DT.

Methods: The modified DKD rat models were induced by uni-nephrectomy, streptozotocin intraperitoneal injection, and a high-fat diet. Following the induction of renal injury, these animals received either SKI, rosiglitazone (ROS), or vehicle, for 42 days. For *in vitro* research, we exposed NRK-52E cells to high glucose (HG) and 4-phenylbutyric acid (4-PBA) with or without SKI or ROS. Changes in parameters related to renal tubular injury and EMT were analyzed *in vivo*. Changes in the proportion of apoptotic renal tubular cells and ER stress, and the signaling pathways involved in these changes, were analyzed both *in vivo* and *in vitro*.

Results: SKI and ROS improved the general condition, the renal morphological appearance and the key biochemical parameters, and attenuated renal injury and EMT in the rat model of DKD. In addition, SKI and ROS alleviated apoptosis, inhibited ER stress, and suppressed PERK-eIF2 α -ATF4-CHOP signaling pathway activation both *in vivo* and *in vitro*. Notably, our

data showed that the regulatory *in vitro* effects of SKI on PERK-eIF2 α -ATF4-CHOP signaling were similar to those of 4-PBA, a specific inhibitor of ER stress.

Conclusion: This study confirmed that SKI can alleviate DT in a similar manner as ROS, and SKI achieves this effect by inhibiting EMT and ER stress-induced apoptosis. Our findings thereby provide novel information relating to the clinical value of SKI in the treatment of DT.

Keywords: diabetic tubulopathy, shenkang injection, apoptosis, renal tubular epithelial mesenchymal transition, endoplasmic reticulum stress

INTRODUCTION

As one of the major microvascular complications of diabetes mellitus (DM), diabetic kidney disease (DKD) has become a common health problem in China (Ma, 2018). Research has shown that 30–40% of patients with DM eventually develop DKD and that this is a dominant cause of end-stage renal disease (Umanath and Lewis, 2018). Although there is now extensive knowledge regarding renal damage in DKD, the pathogenesis of DKD progression remains controversial, especially for patients with early DKD who do not exhibit mass proteinuria (Alicic et al., 2017; Chen et al., 2017). It has been reported that early glomerular disease in DKD triggers a cascade of injuries that result in renal tubulointerstitial disease. An increasing body of *in vivo* and *in vitro* evidence now indicates that the proximal renal tubule plays a critical role in early DKD (Vallon, 2011). This has led to the term diabetic tubulopathy (DT) (Tang et al., 2011). The concept of DT mainly stems from the ability of the proximal tubular epithelial cells (PTECs) to secrete proinflammatory and profibrotic factors and to undergo epithelial mesenchymal transition (EMT) upon stimulation by various metabolic substrates of DM (Zeni et al., 2017). Accordingly, a variety of factors have been detected that have the ability to cause injury to the renal tubules, including interleukin-6 (IL-6), transforming growth factor- β (TGF- β), vascular endothelial growth factor (VEGF) and toll-like receptor 4 (TLR4); several novel pathogenic mechanisms have also been demonstrated in PTECs, including mitochondrial fragmentation, autophagy, and apoptosis (Tang et al., 2010; Alicic et al., 2017; Lee et al., 2019). Consequently, it is highly evident that therapeutic strategies that target DT hold significant promise for patients with early DKD.

Lee et al. (2019) reported that EMT of PTECs is one of the major pathogenic events of DT; this process involves a series of events in which PTECs not only lose several epithelial characteristics including E-cadherin but also acquire typical properties of mesenchymal cells, such as the expression of collagen type I (collagen I), vimentin, and α -smooth muscle actin (α -SMA). In addition, the damage incurred by PTECs during DKD is known to result in the accumulation of unfolded proteins in the endoplasmic reticulum (ER), thus causing a severe unfolded protein response (UPR). Persistent UPR can eventually lead to cellular apoptosis (Cunard, 2015;

Cybulsky, 2017). Therefore, if we are to ameliorate DT, it is vital that we inhibit EMT and ER stress-induced apoptosis in PTECs.

It is well known that three membrane proteins in the ER can function as stress sensors: double-stranded RNA (PKR)-activated protein kinase-like eukaryotic translation initiation factor 2 α (eIF2 α) kinase (PERK), inositol-requiring transmembrane kinase/endoribonuclease 1, and activating transcription factor 6. Normally, these proteins bind to chaperone glucose-regulated protein 78 (GRP78) to form an inactive protein complex. However, under stressful conditions, these protein sensors can be released from the protein complexes to initiate ER stress; this occurs when misfolded proteins accumulate and causes the sequestration of GRP78. PERK, as the ER stress sensor that can phosphorylate eIF2 α , then causes the reduction of protein synthesis and the upregulation of ER stress-related protein expression, including activating transcription factor 4 (ATF4) and C/EBP homologous protein (CHOP). This signaling pathway eventually results in the restoration of cellular homeostasis, particularly with regards to protein translation and folding. The activation of eIF2 α can selectively promote protein translation, thus playing a vital role in ER stress-induced apoptosis. The family of caspase12 and Bcl-2 proteins also play an important role in this signaling pathway (Kitamura, 2008a; Kitamura, 2009; Oakes and Papa, 2015; Oakes, 2020).

Shenkang injection (SKI) has been approved by the National Medical Products Administration for the treatment of chronic kidney disease (CKD) as a modern preparation of Chinese patent medicine (Z20040110) and has been widely used in China to treat renal tubulointerstitial fibrosis (TIF) in patients with CKD for almost 20 years (Song et al., 2019; Zou et al., 2020). In a previous study, Xu et al. reported that SKI, and its major active component emodin, can inhibit the proliferation and apoptosis of mesangial cells induced by high glucose (HG) conditions (Xu et al., 2016). More recently, we also demonstrated that SKI can attenuate TIF *in vivo* by blocking pericyte-myofibroblast transition in the kidneys of rats with obstructive nephropathy (Liu et al., 2019). However, to the best of our knowledge, it is still unknown whether SKI can alleviate DT.

In this study, we used SKI as a new therapeutic strategy to improve EMT and ER stress-induced apoptosis in DT. We compared the effects of SKI to rosiglitazone (ROS), a conventional insulin sensitizing agent that is used in the clinic. In addition to this, we comprehensively evaluated the mechanisms that underlie the beneficial effects of SKI on

diabetic kidneys and PTECs, paying particular attention to the ER stress-related PERK-eIF2 α -ATF4-CHOP signaling pathway.

MATERIALS AND METHODS

Preparation and Quality Control of SKI

SKI was purchased from Xi'an Century Shengkang Pharmaceutical Industry Co., Ltd. (Xi'an, China) and consisted of extracts from a defined mixture of Chinese herbs: radix et rhizoma rhei (*Rheum palmatum* L., Dahuang), radix astragali [*Astragalus membranaceus* (Fisch.) Beg. Huangqi], radix salviae miltiorrhizae (*Salvia miltiorrhiza* Bunge., Danshen), and Flos carthami (*Carthamus tinctorius* L., Honghua). One injection of SKI (20 ml) contains 6 g of extracts in total. The extraction method and the production process for SKI is protected by patent law in China and are both subjected to strict quality control; the main components are also subjected to standardization. The batch number of SKI used in this study was 201,607,021. The quality of the SKI was determined by fingerprint analysis and high performance liquid chromatography (HPLC), as described previously by Yao et al. (2015) and Xu et al. (2017). The main bioactive components of anthraquinones, including *Aloe-emodin* (C₁₅H₁₀O₅; CAS: 481-72-1), *Rhein* (C₁₅H₈O₆; CAS: 478-43-3), *Emodin* (C₁₅H₁₀O₅; CAS: 518-82-1), *Chrysophanol* (C₁₅H₁₀O₄; CAS: 481-74-3), and *Physcion* (C₁₆H₁₂O₅; CAS: 521-61-9) (shown in **Supplemental Figure S1**), exhibited high levels of stability in the products of SKI purchased in different places and used in this study.

Animals and Treatments

Forty-eight male Sprague Dawley rats, weighing 200 \pm 10 g, were provided by the Animal Center of Nanjing Medical University (Nanjing, China). All animal handling and experimental procedures were performed in accordance with local ethics committees and the National Institutes of Health Guide for the Care and Use of Laboratory Animals. All efforts were made to minimize animal suffering and reduce the number of animals used. All procedures involving animals were approved by the Animal Ethics Committee of Nanjing University Medical School (Qualified number: SYXK 2014-0052). The feeding conditions of rats were described previously (Han et al., 2019). The 48 rats were divided into four groups using a random number table, with 5, 14, 14, and 15 rats in the Sham, Vehicle, SKI, and ROS groups, respectively. For rats in the Sham group, the left kidney was exposed during surgery; the rats were then given distilled water and a standard diet for 20 weeks until finished. In contrast, the rats in the other three groups were given a 40% high-fat diet containing 19.8% fat, 22.3% crude protein, and 44.6% carbohydrates, for 4 weeks. The rats in these three groups were then subjected to left nephrectomy and received two intraperitoneal injections (on the right side of their bodies; 3 days apart) of streptozocin (STZ) at a dosage of 35 mg/kg. This process last for 10 weeks and finally established a modified rat model of DKD, as described in detail in our previous studies (Mao et al., 2015; Wu et al., 2017; Wu et al., 2018; Han et al.,

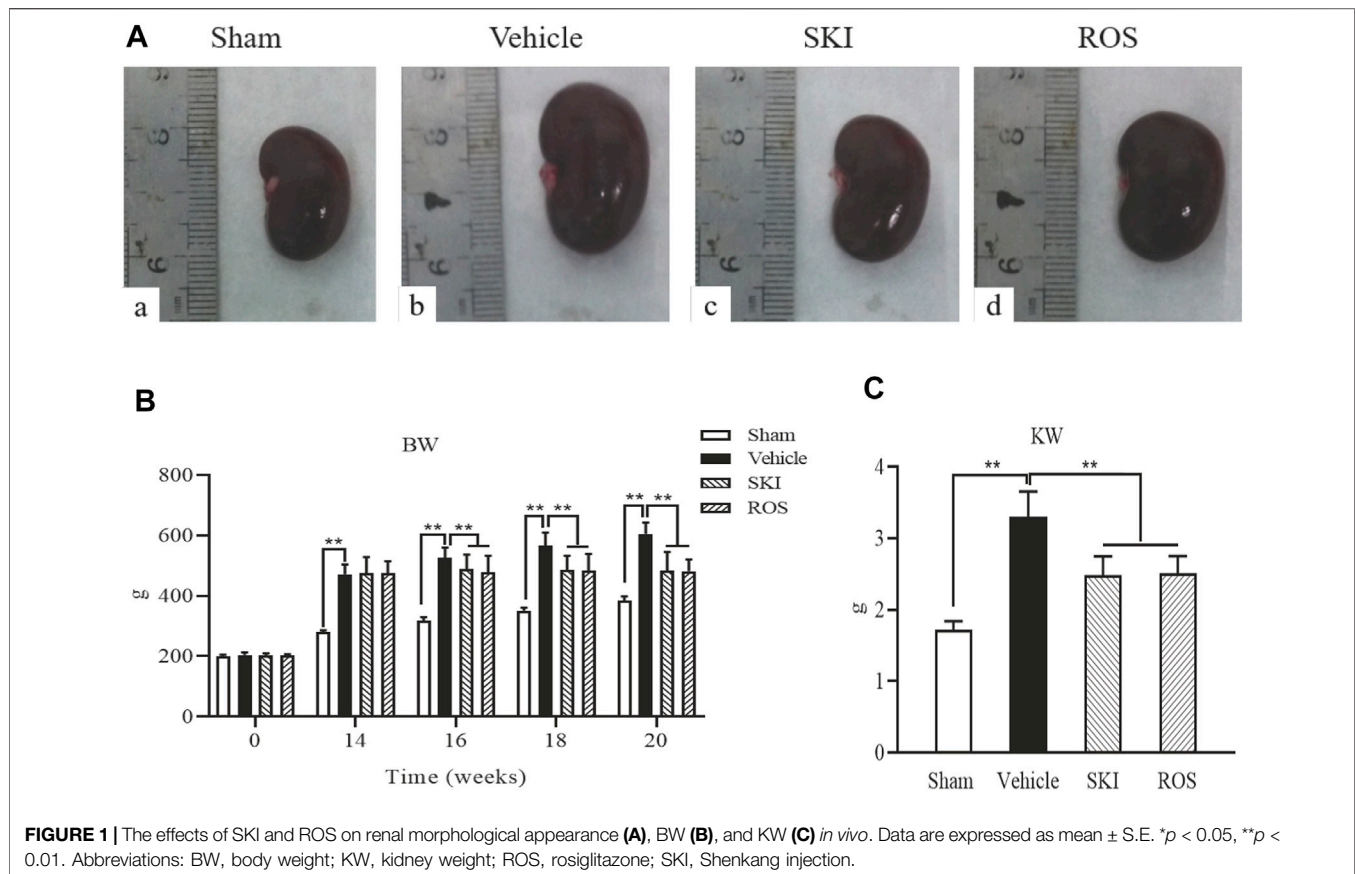
2019). Once the model had been established, we then used gastric gavage to administer appropriate daily treatments: SKI was given to rats in the SKI group, while rats in the Vehicle and ROS groups were treated with 2 ml of distilled water or ROS, respectively. After 6 weeks of treatment with the different interventions, we collected urine firstly, and then anesthetized rats and collected blood, finally sacrificed all rats by cardiac puncture at the same time point. Kidneys were collected for the detection of various indicators; the experimental process is depicted in **Supplemental Figure S2**. In the clinic, 100 ml/day of SKI is normally used to treat a 60 kg non-dialysis patient with CKD. Based on standard animal conversion formulae, the effective amount of SKI in a rat weighing 200 g was determined to be equivalent to 5 g/kg/day. ROS was purchased from GlaxoSmithKline Co. (United Kingdom); the dose used in this experiment (Avandia, 5 mg/kg/day) was used previously by Kang et al. (2013). STZ was obtained from Sigma-Aldrich Chemical Co. (St. Louis, MO, United States).

The General Condition of the Rats and Biochemical Parameters

Each day, we monitored each rat with regards to energy level, diet, water intake, fur color, and general activity. Body weight (BW) and blood glucose (BG) were tested before modeling and every 2 weeks thereafter. The left kidneys of rats in the experimental groups were removed and weighed after cardiac puncture. After 6 weeks of drug intervention, the rats were anesthetized, and blood samples (5 ml) were drawn from the heart. A range of biochemical parameters were tested, including serum albumin (Alb), serum creatinine (Scr), and blood urea nitrogen (BUN). In addition, prior to sacrifice, we collected urinary samples from the four groups and used these samples to detect the ratio of urinary microalbumin to creatinine (UACR) and urinary *N*-acetyl-beta-D-glucosaminidase (UNAG); chromatometry was used to determine these parameters, as described previously (Liu et al., 2019).

Histopathological Analysis, TUNEL Assays, and Immunohistochemistry

Kidney samples were fixed in 4% paraformaldehyde and embedded in paraffin. Then, sections (3 μ m thick) were cut perpendicularly to the long axis of the kidney for histopathological analysis, immunohistochemistry (IHC), and terminal deoxynucleotidyl transferase dUTP nick end labeling (TUNEL) assay. For histopathological analysis, we used Periodic acid-Schiff (PAS) staining and Masson's trichrome staining; stained sections were then investigated by light microscopy (LM). For the TUNEL assay, sections were treated with an *In Situ* Cell Death Detection Kit (Roche, Basel, Switzerland) in accordance with the manufacturer's instructions. For IHC analysis, the paraffin-embedded kidney sections were deparaffinized in xylene and hydrated in a gradient series of alcohol concentrations, followed by water; the sections were subsequently placed in 3% H₂O₂ to eliminate endogenous peroxidase activity. Next, the sections were blocked with



normal goat serum and incubated overnight at 4°C with anti-IL-6, anti-TGF- β , anti-collagen I, anti-vimentin, and anti-GRP78 antibodies (Abcam, Cambridge, United Kingdom). Finally, the sections were stained with a polymer horseradish peroxidase (HRP) detection system (ZSGB-BIO, Beijing, China) and counterstained with hematoxylin. The proportion (%) of positively stained renal tubulointerstitial area across 20 fields of view was then analyzed by Image-Pro Plus (IPP) 5.0 software (Media Cybernetic). Results of pathological analysis were confirmed by a pathologist.

Western Blotting (WB) Analysis: *In Vivo*

WB analysis was performed as described previously (Tu et al., 2020). Renal tissues were isolated using phosphate-buffered saline containing protease inhibitors (PI), and sequentially solubilized with 1% Triton X-100, right inferior phrenic arteries (RIPA) buffer (0.1% sodium dodecyl sulfate (SDS), 1% sodium deoxycholate, 1% Triton X-100, 0.15 mol/L NaCl, and 0.01 mol/L ethylenediaminetetraacetic acid in 0.025 mol/L Tris-HCl, pH 7.2) with PI, and separated into Triton X-100-soluble (T), RIPA-soluble (R), and RIPA-insoluble (S) fractions. The RIPA-insoluble fraction was solubilized with sodium dodecyl sulfate-polyacrylamide gel electrophoresis (SDS-PAGE) sample buffer (2% SDS, 10% glycerol, and 5% 2-mercaptoethanol in 0.0625 mol/L Tris-HCl, pH 6.8) (S fractions). Equal amounts of these sequentially solubilized fractions were subjected to SDS-PAGE with 7.5% or 10% acrylamide

gels and then transferred onto a polyvinylidene fluoride membrane (Bio-Rad, Hercules, CA, United States) by electrophoretic transblotting for 30 min using a Trans-Blot SD system (Bio-Rad). After blocking with bovine serum albumin (BSA), the strips of membrane were exposed to anti-IL-6, TGF- β , VEGF, TLR4, α -SMA, vimentin, collagen I, Bax, Bcl-2, caspase12, GRP78, p-PERK, PERK, p-eIF2 α , eIF2 α , ATF4, CHOP, and glyceraldehyde-3-phosphate dehydrogenase (GAPDH) antibodies (Abcam, Cambridge, United Kingdom). Subsequently, these strips were washed and incubated with peroxidase-conjugated secondary antibodies for 1 h at room temperature. Finally, the bands were visualized by an alkaline phosphatase chromogen kit (5-bromo-4-chloro-3-indolyl phosphate p-toluidine salt/nitro blue tetrazolium; Biomedica, AG, Staad, Switzerland). The density of the positive bands was quantified by densitometry (ATTO, Tokyo, Japan). Next, we determined the ratio of the densitometric signal of the target molecule to that of GAPDH.

Cell Culture and Treatment

NRK-52E cells, a murine PTECs line, were kindly provided by Dr. Jian Yao (University of Yamanashi, Chuo, Japan) and cultured as described previously (Liu et al., 2018; Tu et al., 2020). In brief, the NRK-52E cells were cultured in Dulbecco's modified Eagle's medium/Ham's F-12 (HyClone) supplemented with 5% fetal bovine serum (FBS; Gibco, Grand Island, NY, United States). The NRK-52E cells were then exposed to HG (30 mmol/L D-glucose) and 4-phenylbutyric acid (4-PBA, 5 mmol/L, ER

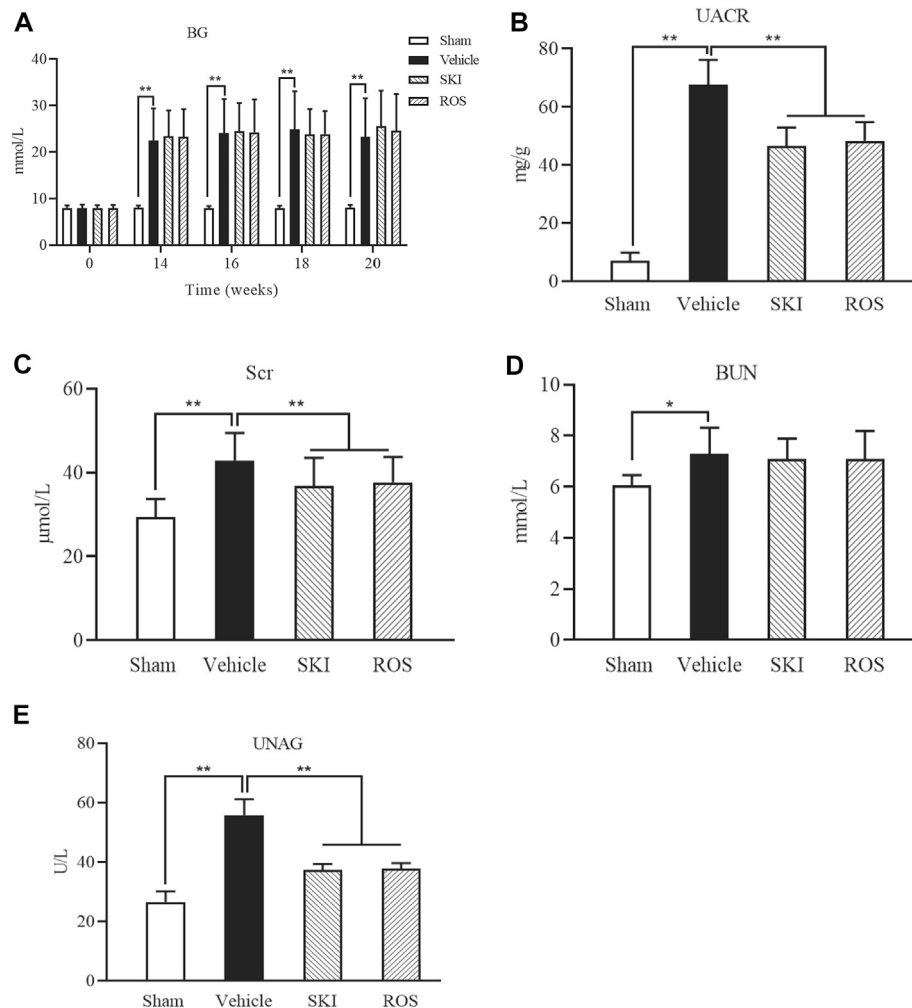


FIGURE 2 | The effects of SKI and ROS on BG (A), UACR (B), Scr (C), BUN (D), and UNAG (E) *in vivo*. Data are expressed as mean \pm S.E. $**p < 0.01$. Abbreviations: BG, blood glucose; UACR, urinary microalbumin to creatinine; Scr, serum creatinine; BUN, blood urea nitrogen; UNAG, urinary *N*-acetyl-beta-D-glucosaminidase; ROS, rosiglitazone; SKI, Shenkang injection.

stress inhibitor) with or without SKI at a concentration of 20 $\mu\text{g}/\text{ml}$ or ROS at a concentration of 10 mmol/L for 24 h. For this experiment, the concentrations of SKI, ROS, and 4-PBA were described by Xu et al. (2016), Kang et al. (2013), and Min et al. (2018), respectively.

Cell Viability Assessment

The viability of NRK-52E cells was assessed by the CCK-8 Kit (Beyotime, Shanghai, China). The cells were seeded into 96-well plates, with three replicate wells for each group, at a density of 1×10^4 cells per well, with 100 μl of medium. After the cells were incubated for the indicated time period, 10 μl of CCK-8 solution was added to each well, followed by incubation for 2 h. The optical density (OD) was then determined at an absorbance of 450 nm, and the cell viability was calculated.

WB Analysis: *In Vitro*

NRK-52E cells were administered with appropriate treatments for 24 h, respectively. Following treatment, cell lysates were separated by gel electrophoresis and blotted with antibodies against Bax, Bcl-2, caspase12, GRP78, p-PERK, PERK, p-eIF2 α , eIF2 α , ATF-4, CHOP, and GAPDH. The secondary antibody was HRP-conjugated anti-rabbit IgG antibody. WB analysis was then carried out on samples of cells from each group; for this, we used a protocol described in our previous publications (Tu et al., 2020; Liu et al., 2021).

Statistical Analysis

The WB assessment was repeated at least thrice independently, and the individual data were subjected to a densitometric analysis. The data are expressed as the means \pm standard deviation. The statistical analysis was performed by one way analysis of variance (ANOVA) on normally distributed data, with least significant difference (LSD) post-

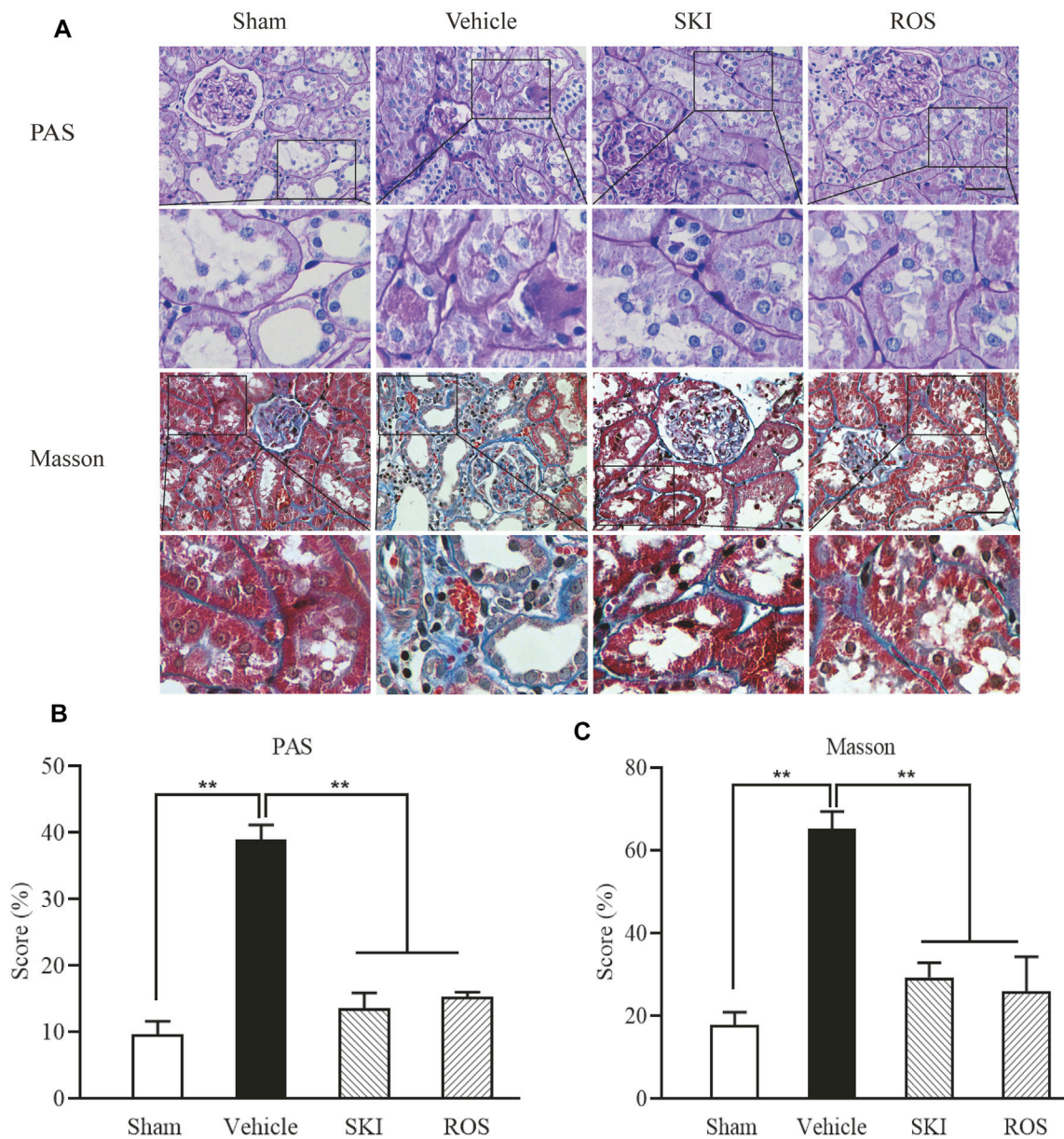


FIGURE 3 | The effects of SKI and ROS on tubulointerstitial pathological changes *in vivo*. **(A)** PAS and Masson staining in the kidney ($\times 200$); **(B)** The rate of ECM/interstitial area; **(C)** The rate of collagen/interstitial area. Scale bar = 100 μm . Data are expressed as mean \pm S.E. $**p < 0.01$. Abbreviations: PAS, Periodic acid-Schiff; ECM, extracellular matrix; ROS, rosiglitazone; SKI, Shenkang injection.

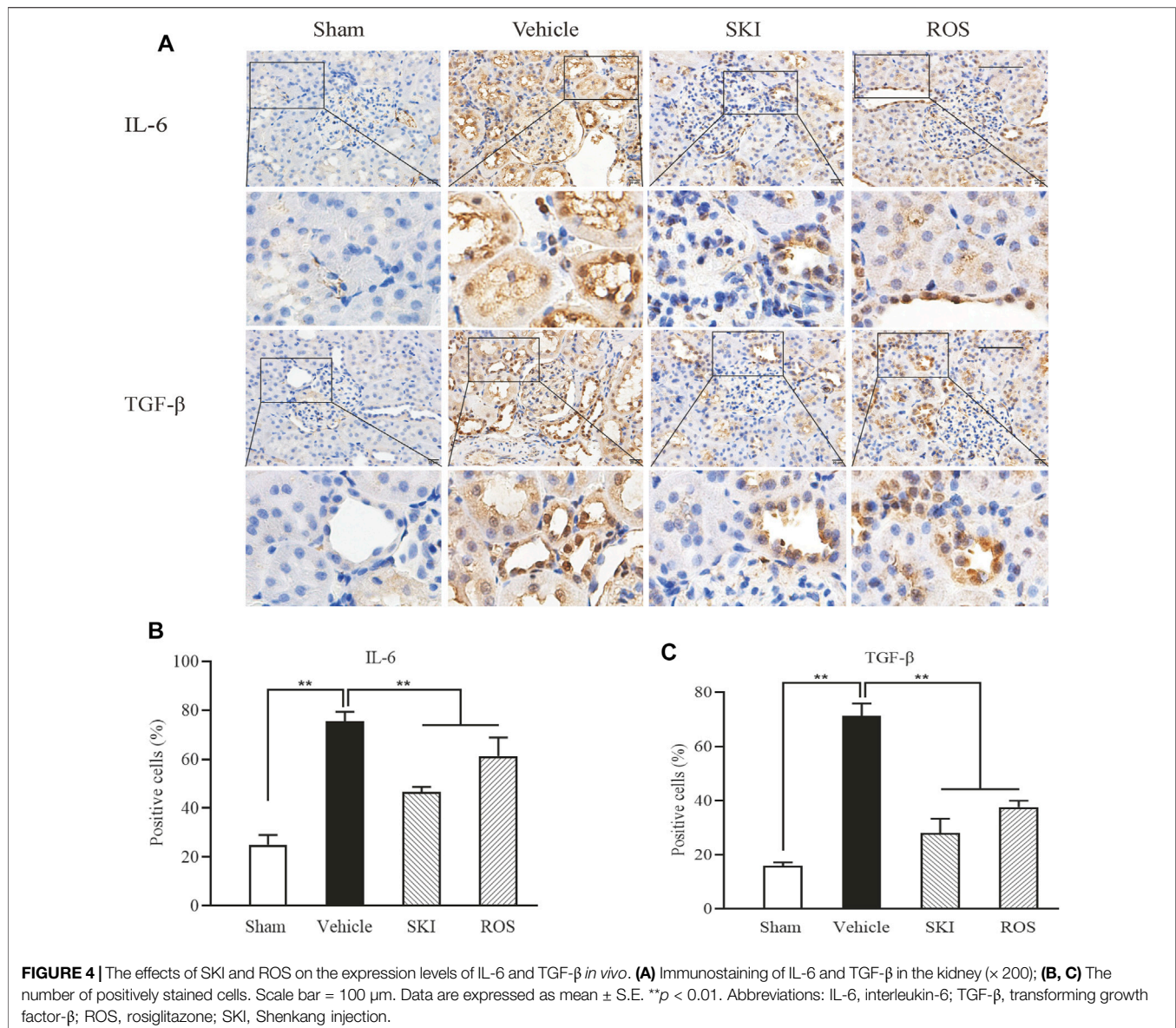
hoc test, or non-parametric Kruskal-Wallis if not. A p -value < 0.05 indicated a statistically significant difference.

RESULTS

General Conditions, Renal Morphology, and Biochemical Parameters in the Rat Model of DKD Were all Improved by SKI and ROS

First, we compared the effects of SKI and ROS on the general condition, renal morphology, BW, and kidney weight (KW), in

the rat model of DKD. Except for the Sham group of rats, the animals in the other three groups exhibited polyuria, polydipsia, polyphagia, low activity, dull fur, and BW gain; these effects occurred to differing degrees. The rats in the Vehicle group showed the most obvious effects. As shown in **Figure 1**, after sacrifice, we found that the kidneys of rats in the Sham group were moderated, while the kidneys of rats in the Vehicle group were swollen. The kidneys of rats treated with SKI or ROS were significantly ameliorated (for example, exhibited reduced less swelling and ischemia) when compared with rats from the Vehicle group (**Figure 1A**). In addition, the BW and KW of rats in the Vehicle group was obviously higher than those in the



Sham group. The BW and KW of rats in the SKI and ROS groups was lower than those of rats in the Vehicle group (**Figures 1B,C**).

Next, we compared the effects of SKI and ROS on BG and UACR in the DKD model rats. As shown in **Figure 2**, following the induction of renal injury, the levels of BG in the Vehicle group rats increased and were maintained at high levels by consecutive subcutaneous injections of Novolin N. Furthermore, the levels of BG in the SKI and ROS groups of rats also remained at high levels following the induction of renal injury for 6 weeks. There were no significant differences in the levels of BG when compared between the SKI and ROS groups of rats (**Figure 2A**). Moreover, 6 weeks after the induction of renal injury, the levels of UACR of rats in the Vehicle group had reached an abnormal level of 67.79 ± 8.35 mg/g; these were significantly higher than those in the

Sham group of rats. After the treatment with SKI or ROS for 6 weeks, the levels of UACR in the SKI and ROS group rats were significantly lower than those in rats from the Vehicle group (**Figure 2B**).

Next, we investigated the effects of SKI and ROS on BUN, Scr, and UNAG, in the rat model of DKD. As shown in **Figure 2**, 6 weeks after the induction of renal injury, the levels of BUN, Scr, and UNAG in the Vehicle group were significantly higher than those in the Sham group. Following 6 weeks of SKI and ROS treatment, the levels of Scr and UNAG in the rat model of DKD were significantly lower than those in the Vehicle group of rats. However, the levels of BUN in the SKI and ROS groups of rats did not change significantly after SKI or ROS treatment (**Figures 2C-E**).

These data indicated that SKI and ROS partially improved the general condition, renal morphology, and biochemical

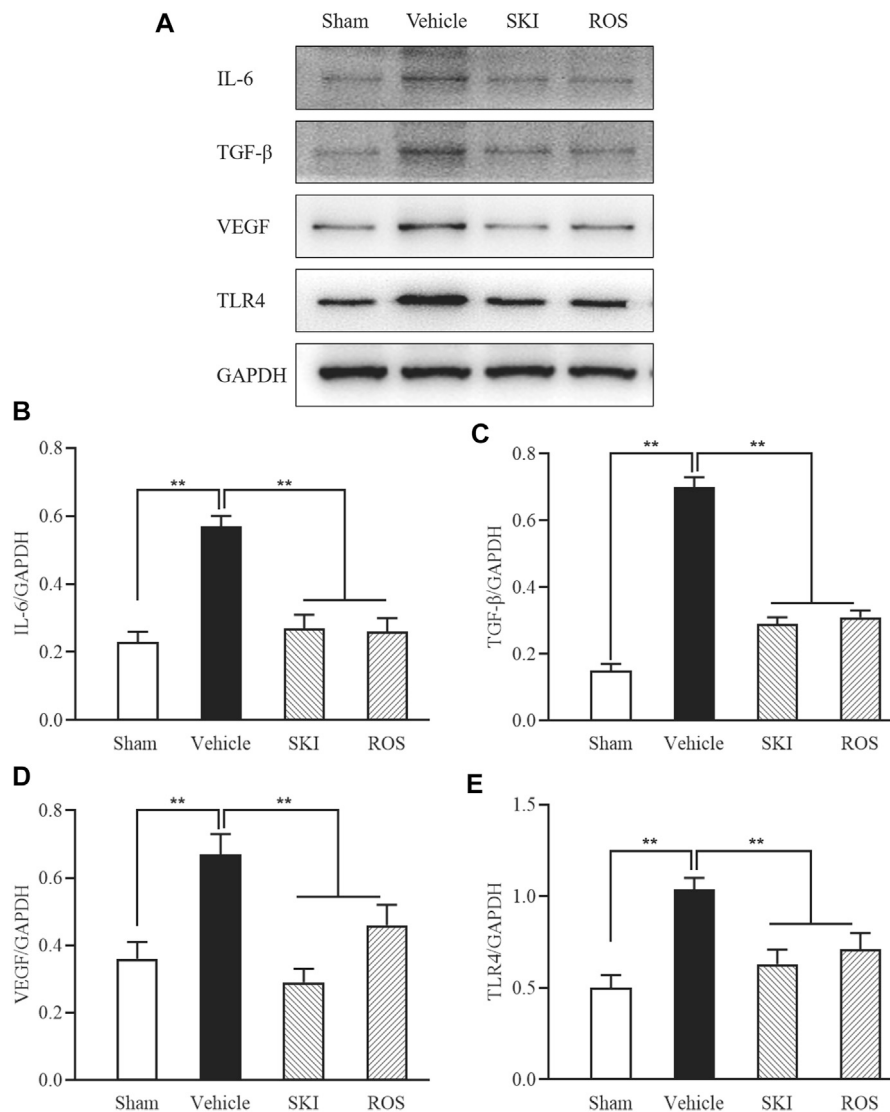


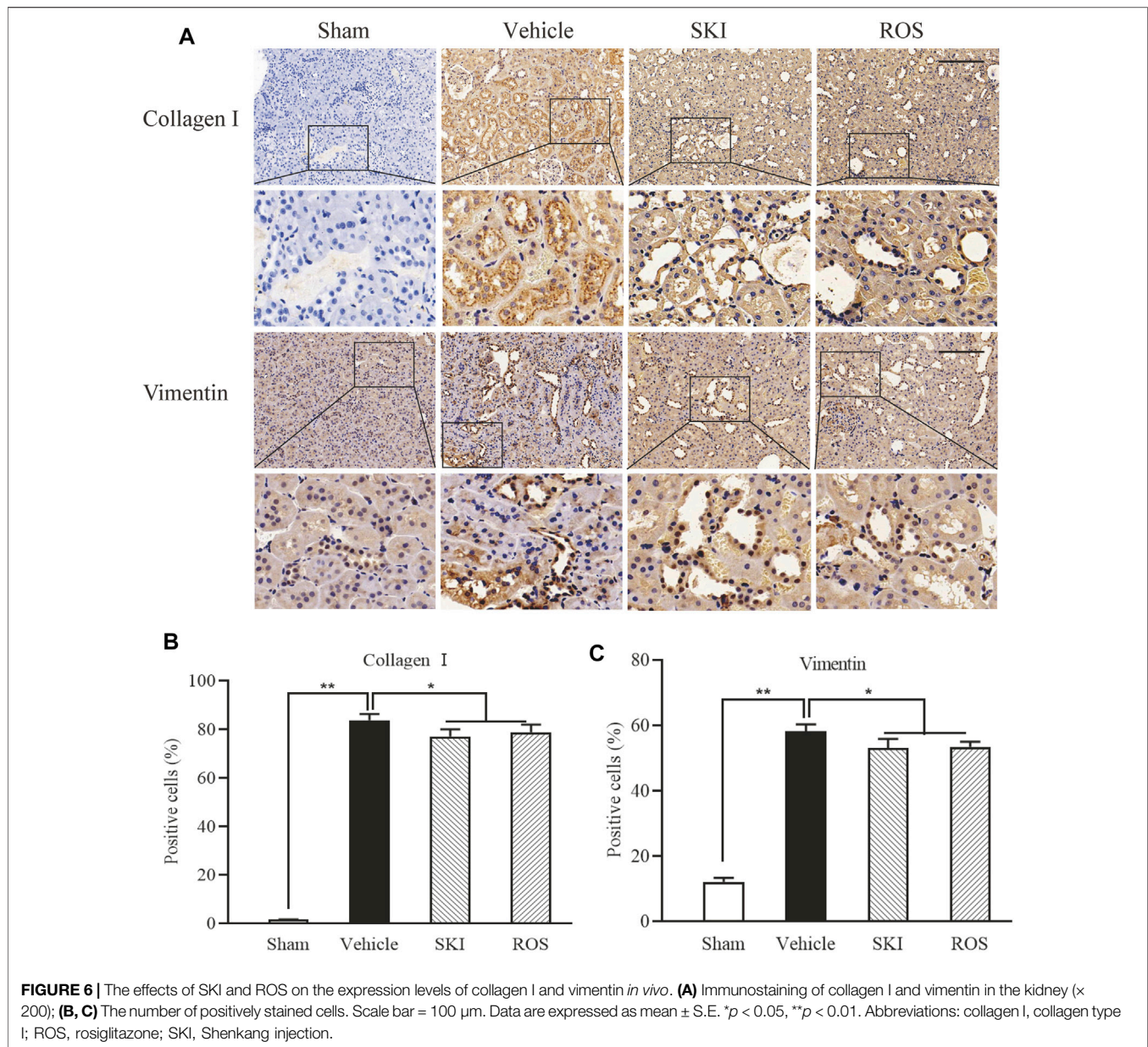
FIGURE 5 | The effects of SKI and ROS on the protein expression levels of IL-6, TGF- β , VEGF, and TLR4, *in vivo*. **(A)** WB analysis of IL-6, TGF- β , VEGF, and TLR4, in the kidney; **(B–E)** The rate of IL-6, TGF- β , VEGF, and TLR4 to GAPDH, respectively. Data are expressed as mean \pm S.E. ** $p < 0.01$. Abbreviations: IL-6, interleukin-6; TGF- β , transforming growth factor- β ; VEGF, vascular endothelial growth factor; TLR4, toll-like receptor 4; GAPDH, glyceraldehyde-3-phosphate dehydrogenase; ROS, rosiglitazone; SKI, Shenkang injection.

parameters of the rat model of DKD, including BW, KW, UACR, Scr, and UNAG.

Renal Tubular Injury in the Rat Model of DKD Was Ameliorated by SKI and ROS

Next, we investigated the effects of SKI and ROS on tubulointerstitial pathological changes in the rat model of DKD. As shown in **Figure 3**, 6 weeks after the induction of renal injury, LM showed that there were obvious pathological changes in the Vehicle group of rats when compared to those in the Sham group, including epithelial cell edema and

hypertrophy, vacuolar lesions in the renal tubules, tubular obliteration, and irregular morphology; we also observed slight deposition of collagen in the renal interstitium. After 6 weeks of SKI or ROS treatment, the degree of tubulointerstitial pathological changes in the rat model of DKD were significantly improved when compared to those in the Vehicle group, including epithelial cell edema and hypertrophy, vacuolar lesions in the renal tubules, tubular obliteration and irregular morphology, and collagen deposition in the renal interstitium. Notably, we did not observe obvious extracellular matrix (ECM) accumulation in the renal interstitium in the DKD rats.



Next, we investigated the effects of SKI and ROS on the expression levels of a range of injury markers in the renal tubules of DKD model rats by IHC staining and WB analysis, including IL-6, TGF- β , VEGF, and TLR4. As shown in **Figures 4, 5**, compared with the Sham group of rats, 6 weeks after the induction of renal injury, we observed significant immunostaining of IL-6 and TGF- β in the renal tubular epithelial cells and increased protein levels of IL-6, TGF- β , VEGF, and TLR4 in the kidneys of the Vehicle group rats. Compared to rats in the Vehicle group, those in the SKI and ROS groups showed significant reductions in these parameters after 6 weeks of the treatment.

Collectively, these data indicated that SKI and ROS significantly ameliorated various aspects of renal tubular injury in the rat model of

DKD, including tubulointerstitial pathological changes and the expression levels of various markers of renal tubular injury.

Renal Tubular EMT in the Rat Model of DKD Was Attenuated by SKI and ROS

Next, we used IHC and WB analysis to investigate the effects of SKI and ROS on various markers of renal tubular EMT, including E-cadherin, collagen I, vimentin, and α -SMA in the kidneys of DKD rats. As shown in **Figures 6, 7**, 6 weeks after the induction of renal injury, compared with the Sham group of rats, there was obvious immunostaining of collagen I and vimentin in the renal tubular epithelial cells of rats in the Vehicle group. This was accompanied by increased protein expression levels of collagen I,

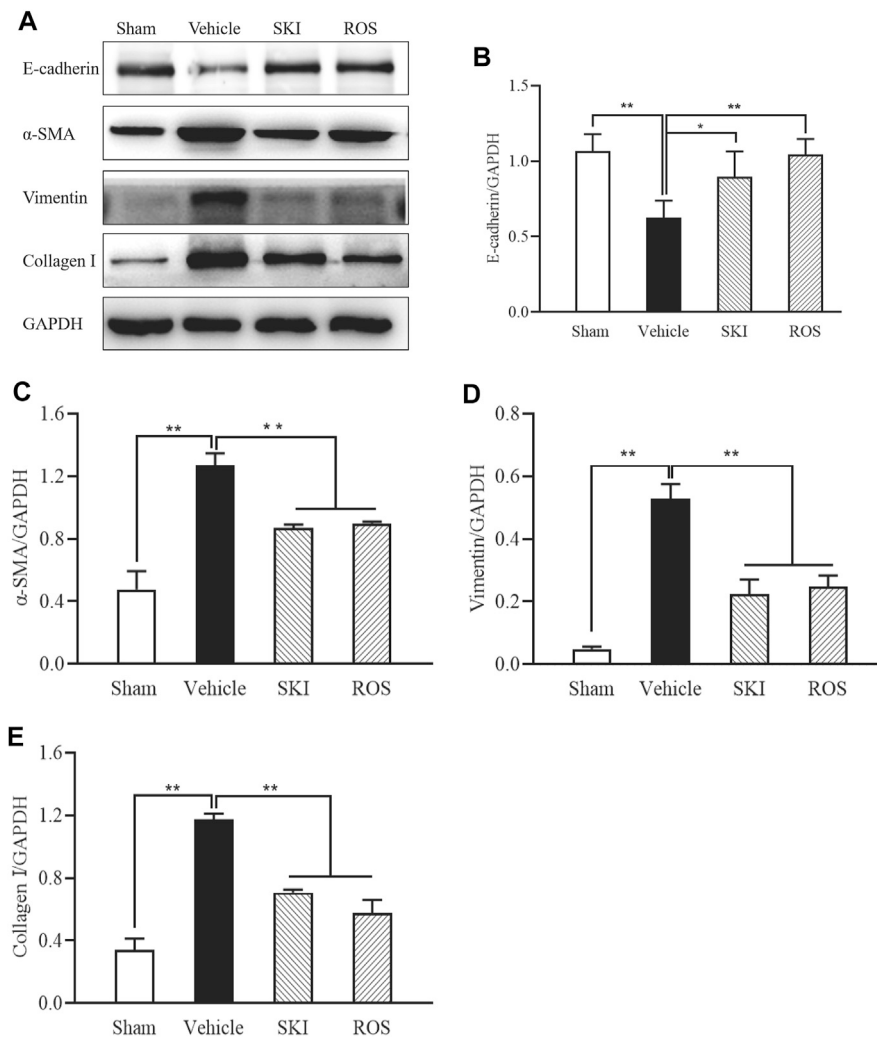


FIGURE 7 | The effects of SKI and ROS on the protein expression levels of E-cadherin, α -SMA, vimentin, and collagen I, *in vivo*. **(A)** WB analysis of α -SMA, vimentin, and collagen I, in the kidney; **(B–E)** The rate of α -SMA, vimentin, and collagen I to GAPDH, respectively. Data are expressed as mean \pm S.E. $**p < 0.01$. Abbreviations: α -SMA, α -smooth muscle actin; collagen I, collagen type I; WB, Western blot; GAPDH, glyceraldehyde-3-phosphate dehydrogenase ROS, rosiglitazone; SKI, Shenkang injection.

vimentin, and α -SMA, as well as decreased protein expression level of E-cadherin in the kidneys. There were significant reversions in these parameters in the SKI and ROS groups of rats after 6 weeks of SKI or ROS treatment when compared to those of the Vehicle group of rats.

These data showed that SKI and ROS significantly attenuated renal tubular EMT in the rat model of DKD.

Apoptosis in the Renal Tubular Cells Was Alleviated by SKI and ROS *in Vivo* and *in Vitro*.

Next, we used TUNEL staining and WB analysis to investigate the effects of SKI and ROS on apoptosis in the renal tubular cells as indicated by staining in the renal tubular epithelial cells and changes in the protein

expression levels of Bax, Bcl-2, and caspase12 in the kidneys of the rat model of DKD. As shown in **Figures 8, 9**, 6 weeks after the induction of renal injury, compared with the Sham group of rats, there was obvious TUNEL staining of the renal tubular epithelial cells in the Vehicle group of rats, along with increased protein expression levels of Bax and caspase12; the level of Bcl-2 was significantly reduced in the kidneys of the Vehicle group of rats. These parameters all showed significant improvement in the SKI and ROS groups of rats after 6 weeks of the treatment when compared to those of the Vehicle group of rats.

To investigate whether SKI and ROS can reduce apoptosis in the renal tubular cells *in vitro*, we determined the protein expression levels of Bax, Bcl-2, and caspase12 in NRK-52E cells exposed to HG with or without SKI or ROS for 24 h. Prior to the formal cellular experiments, we determined the

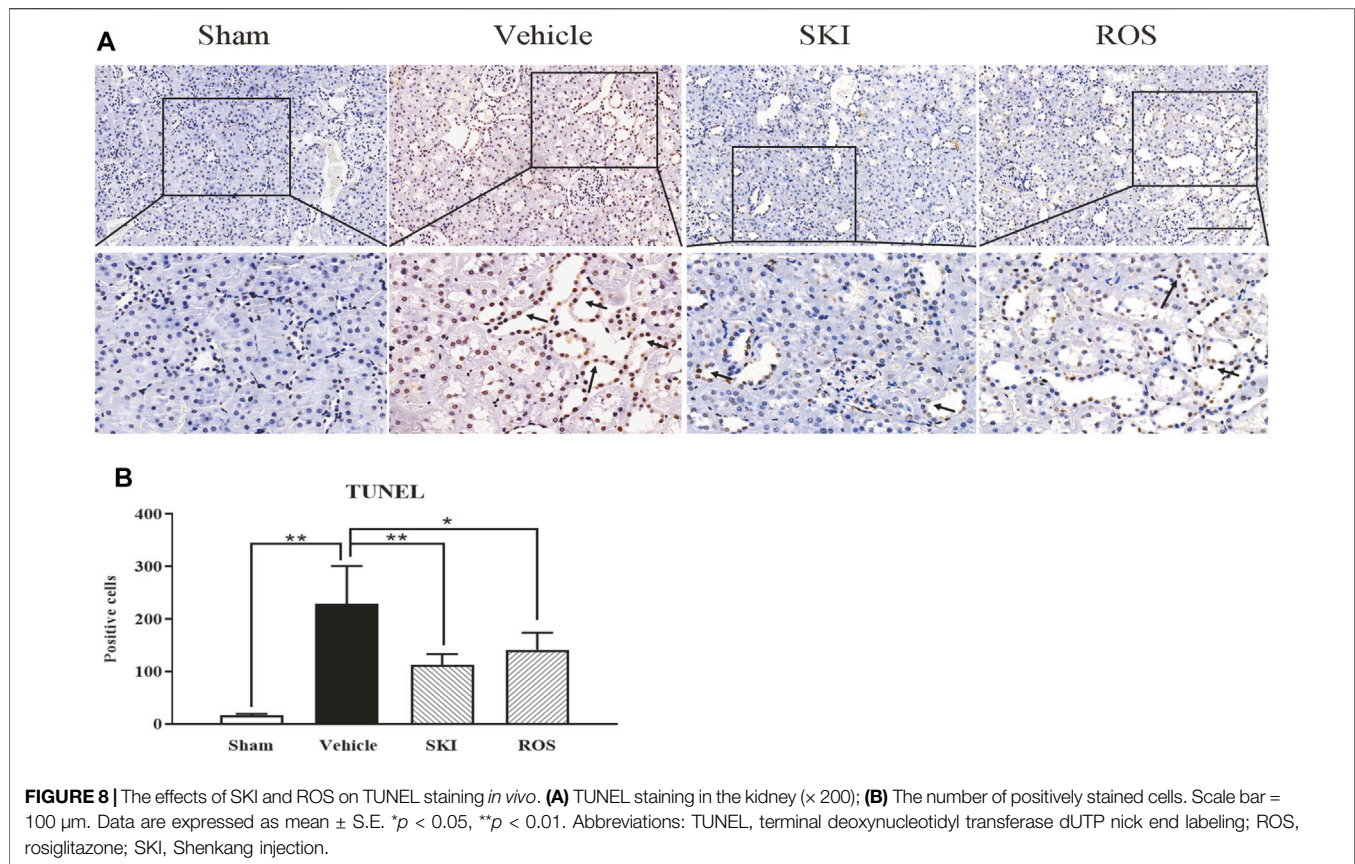


FIGURE 8 | The effects of SKI and ROS on TUNEL staining *in vivo*. **(A)** TUNEL staining in the kidney ($\times 200$); **(B)** The number of positively stained cells. Scale bar = 100 μm . Data are expressed as mean \pm S.E. * $p < 0.05$, ** $p < 0.01$. Abbreviations: TUNEL, terminal deoxynucleotidyl transferase dUTP nick end labeling; ROS, rosiglitazone; SKI, Shenkang injection.

cytotoxicity of SKI or ROS on NRK-52E cells with a CCK-8 kit. As shown in **Supplemental Figure S3**, cellular viability was significantly reduced when treated with higher concentrations of SKI (40 $\mu\text{g}/\text{ml}$) and ROS (200 nmol/L) when compared to a 20 $\mu\text{g}/\text{ml}$ concentration of SKI and a 100 nmol/L concentration of ROS. Based on these results, we selected safe and effective concentrations for both SKI (20 $\mu\text{g}/\text{ml}$) and ROS (100 nmol/L). **Figure 10** shows that the protein expression levels of Bax and caspase 12 were significantly higher, while the level of Bcl-2 was significantly lower in NRK-52E cells exposed to HG when compared to control cells. The treatment with SKI or ROS significantly ameliorated these changes in NRK-52E cells exposed to HG when compared to HG treatment alone. In addition, we also observed improvements in the protein expression levels of Bax, Bcl-2, and caspase12 in NRK-52E cells exposed to HG and 4-PBA (an inhibitor of ER stress) when compared to cells treated with HG alone.

Collectively, these data showed that SKI and ROS alleviated apoptosis in the renal tubular cells both *in vivo* and *in vitro*.

ER Stress in Renal Tubular Cells Was Inhibited by SKI and ROS *in Vivo* and *in Vitro*

ER stress is an important factor that acts upstream of apoptosis (Kitamura, 2008b; Kitamura, 2009). Therefore, we evaluated the expression of GRP78 as a marker of ER stress in the kidneys of DKD rats by IHC staining and WB analysis. As shown in

Figure 11, 6 weeks after the induction of renal injury, compared with the Sham group of rats, there was obvious GRP78 immunostaining in the renal tubular epithelial cells and increased protein expression levels of GRP78 in the kidneys of the Vehicle group. SKI and ROS treatment led to a significant reduction in these effects when compared to those in the Vehicle group.

Next, we tested the protein expression level of GRP78 in NRK-52E cells exposed to HG with or without SKI or ROS for 24 h. **Figure 11** shows that when compared with control cells, the NRK-52E cells exposed to HG exhibited significantly higher expression levels of GRP78 protein; when treated with SKI or ROS, NRK-52E cells exposed to HG exhibited a significant reduction in the levels of GRP78 protein when compared to HG treatment alone. In addition, we observed that the protein expression level of GRP78 was lower in NRK-52E cells exposed to HG and 4-PBA than those treated with HG alone.

These data showed that SKI and ROS inhibited renal tubular ER stress *in vivo* and *in vitro*.

Activation of the PERK-eIF2 α -ATF4-CHOP Signaling Pathway Was Suppressed by SKI and ROS *in Vivo* and *in Vitro*.

PERK-eIF2 α -ATF4-CHOP signaling is an important regulatory mechanism in ER stress (Kitamura, 2008a; Kang et al., 2017). Thus, we used WB analysis to investigate the expression levels of

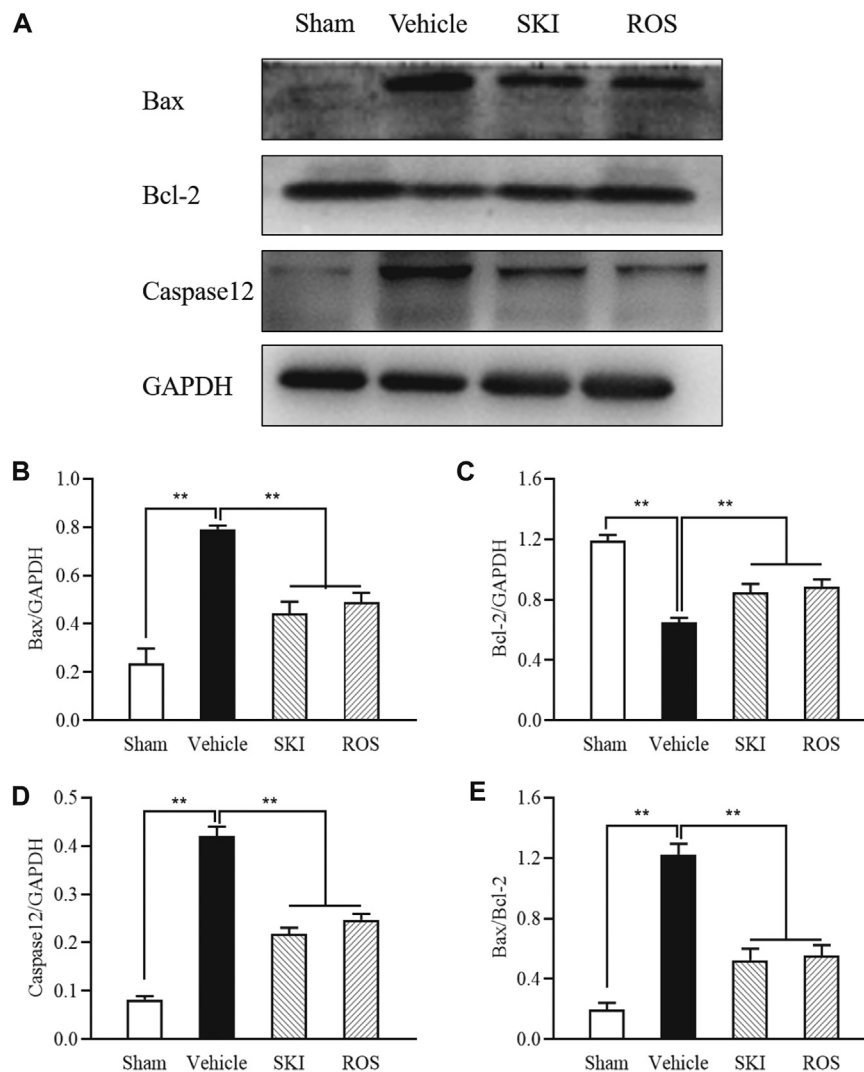


FIGURE 9 | The effects of SKI and ROS on the protein expression levels of Bax, Bcl-2, and caspase12, *in vivo*. **(A)** WB analysis of Bax, Bcl-2, and caspase12, in the kidney; **(B–E)** The rate of Bax, Bcl-2 and caspase12 to GAPDH, respectively, and the rate of Bax to Bcl-2. Data are expressed as mean \pm S.E. ** $p < 0.01$. Abbreviations: WB, Western blot; GAPDH, glyceraldehyde-3-phosphate dehydrogenase; ROS, rosiglitazone; SKI, Shenkang injection.

key signaling molecules in the renal PERK-eIF2 α -ATF4-CHOP pathway. **Figure 12** shows that the protein expression levels of p-PERK, p-eIF2 α , ATF4, and CHOP, in the kidneys of the Vehicle group of rats were significantly higher than those in the Sham group of rats. In comparison with the Vehicle group of rats, those in the SKI or ROS groups exhibited significant reductions in the protein expression levels of p-PERK, p-eIF2 α , ATF4, and CHOP, in the kidneys.

Figure 13 shows that the protein expression levels of p-PERK, p-eIF2 α , ATF4, and CHOP, in NRK-52E cells exposed to HG were significantly higher than those in the control cells. In comparison with HG treatment alone, the protein expression levels of p-PERK, p-eIF2 α , ATF4, and CHOP, in NRK-52E cells exposed to SKI or ROS were all significantly lower. In addition, we also observed significantly lower protein expression levels of

p-PERK, p-eIF2 α , ATF4, and CHOP, in NRK-52E cells exposed to HG and 4-PBA than those treated with HG alone.

These data showed that SKI and ROS suppressed activation of the PERK-eIF2 α -ATF4-CHOP signaling pathway, both *in vivo* and *in vitro*.

DISCUSSION

In 1999, Gilbert and Cooper proposed the non-glomerular mechanisms that may be involved in the tubular injury caused by DM and emphasized that the renal tubulointerstitial damage was more extensive in such cases than could be explained by glomerular disease alone (Gilbert and Cooper, 1999). An increasing body of evidence now suggests a primary role for

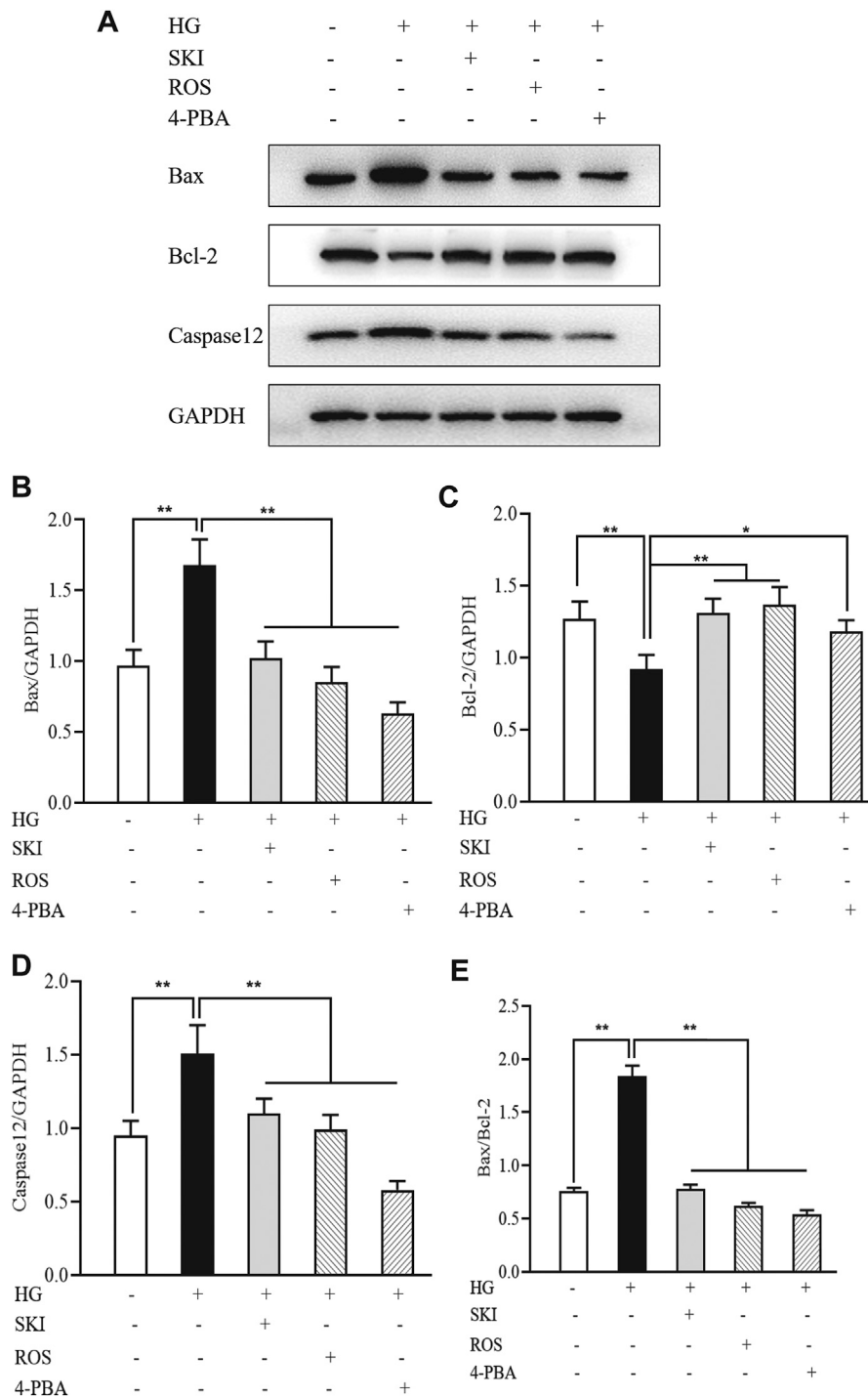


FIGURE 10 | The effects of SKI and ROS on the protein expression levels of Bax, Bcl-2, and caspase12, *in vitro*. **(A)** WB analysis of Bax, Bcl-2, and caspase12, in NRK-52E cells exposed to HG and 4-PBA with or without SKI or ROS for 24 h; **(B–E)** The rate of Bax, Bcl-2, and caspase12, to GAPDH, respectively, and the rate of Bax to Bcl-2. Data are expressed as mean \pm S.E. * $p < 0.05$, ** $p < 0.01$. Abbreviations: WB, Western blot; HG, high glucose; 4-PBA, 4-phenylbutyric acid; GAPDH, glyceraldehyde-3-phosphate dehydrogenase; ROS, rosiglitazone; SKI, Shenkang injection.

PTECs in the creation of lesions and dysfunction in the kidney nephrons, and has led to this condition being referred to by the independent term diabetic tubulopathy or “DT” (Tang et al.,

2011; Vallon, 2011). At present, it is generally accepted that hyperglycemia is an important causative factor in the pathogenesis of DKD and that this condition exerts both

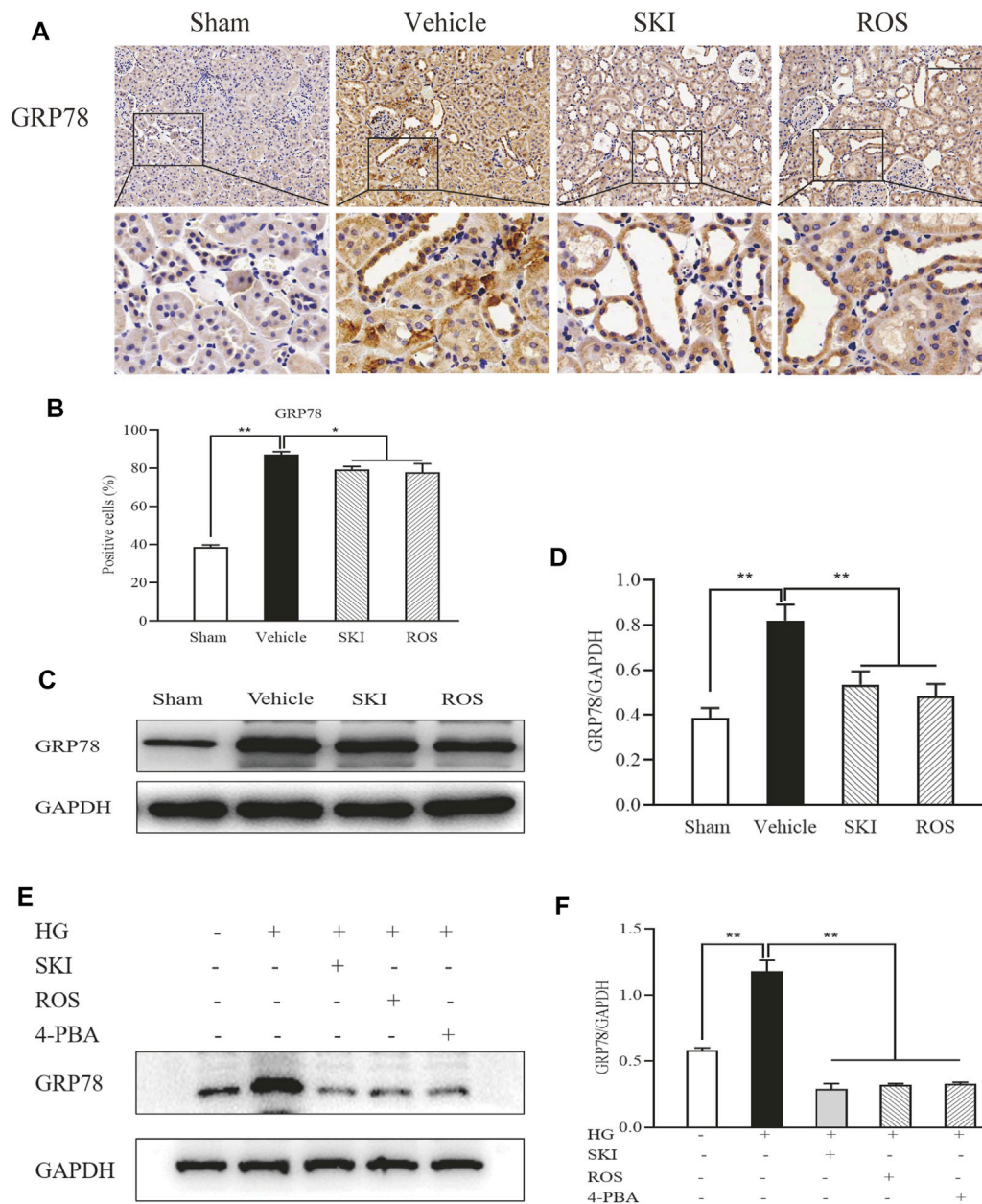
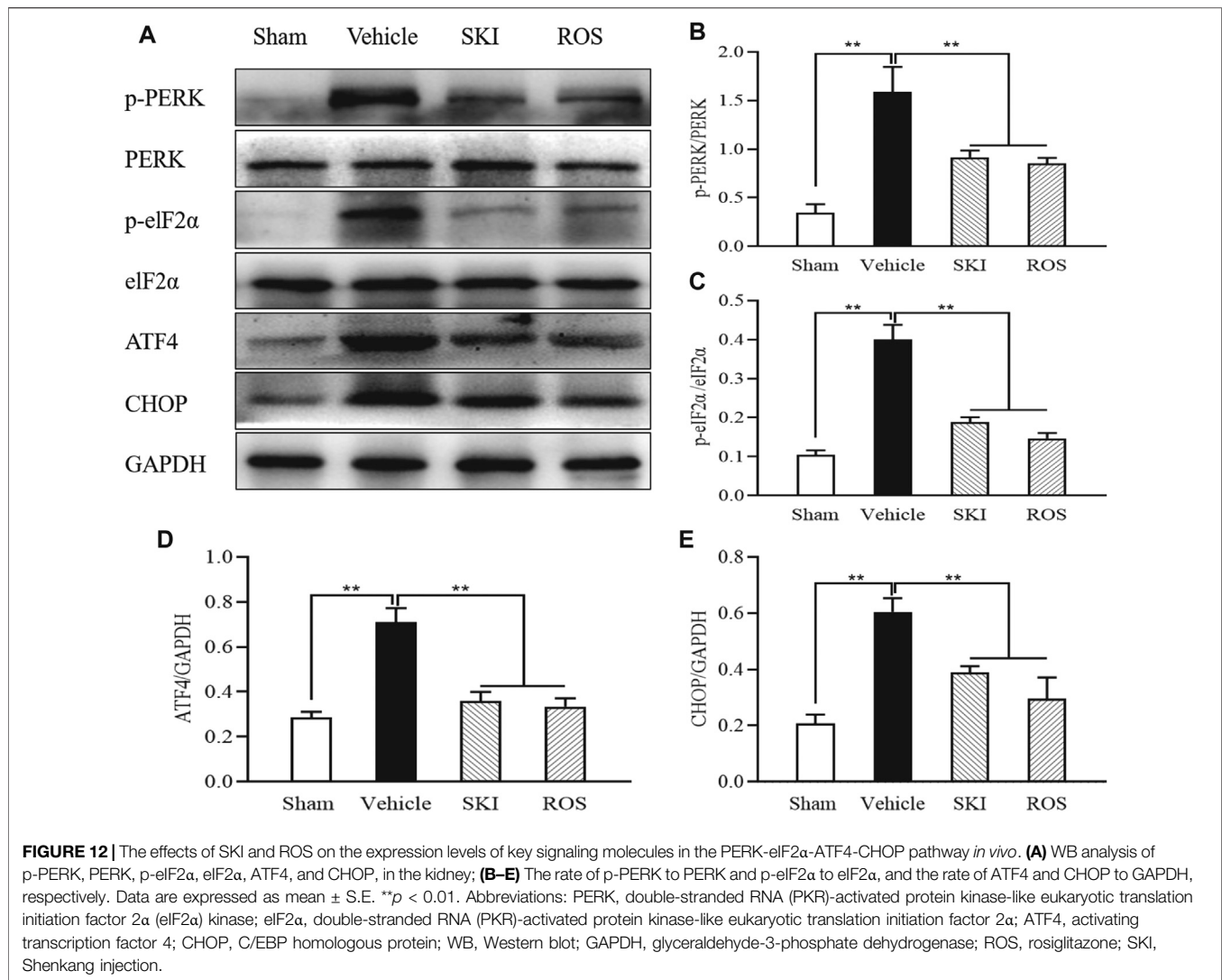


FIGURE 11 | The effects of SKI and ROS on the expression levels of GRP78 *in vivo* and *in vitro*. **(A)** Immunostaining of GRP78 in the kidney ($\times 200$); **(B)** The number of positively stained cells; **(C)** WB analysis of GRP78 in the kidney; **(D)** The rate of GRP78 to GAPDH; **(E)** WB analysis of GRP78 in NRK-52E cells exposed to HG and 4-PBA with or without SKI or ROS for 24 h. **(F)** The rate of GRP78 to GAPDH. Scale bar = 100 μm . Data are expressed as mean \pm S.E. * $p < 0.05$, ** $p < 0.01$. Abbreviations: GRP78, glucose-regulated protein 78; WB, Western blot; GAPDH, glyceraldehyde-3-phosphate dehydrogenase; HG, high glucose; 4-PBA, 4-phenylbutyric acid; ROS, rosiglitazone; SKI, Shenkang injection.

proinflammatory and profibrotic effects on PTECs. *In vitro* and *in vivo* studies have shown that the exposure of PTECs to HG conditions promotes proinflammatory, profibrotic, and angiogenic responses that are associated with tubulointerstitial pathological changes and the overexpression of several deleterious factors in the renal tubules, including IL-6, TGF- β , VEGF, and TLR4 (Alicic et al., 2017; Chen et al., 2017). Therefore, in this study, we first tried to establish a rat model of DKD that

involved renal tubular injury. Our results showed that we successfully established a rat model of DKD and that these animals exhibited hyperglycemia; expressed abnormal levels of UACR and UNAG; expressed increased levels of Scr and BUN; and exhibited obvious tubulointerstitial pathological changes, including epithelial cell edema and hypertrophy, renal tubular vacuolar lesions, tubular obliteration and irregular morphology, and slight deposition of collagen in the renal interstitium.



Furthermore, more importantly, we detected significantly higher expression levels of IL-6, TGF- β , VEGF, and TLR4 in the kidneys of these DKD rat models; these factors are all known to cause deleterious effects in terms of kidney function. We thereby considered that our rat model of DKD should be helpful to understand the mechanisms underlying tubular injury and to identify novel therapeutic drugs for DT.

In our previous studies, we reported that SKI, a modern preparation of Chinese patent medicine, was able to reduce TIF in obstructive nephropathy (Liu et al., 2019). In the present study, we established a rat model of DKD with tubular injury by performing unilateral nephrectomy and injecting STZ. Following the induction of renal injury, we treated the DKD model rats for 6 weeks with SKI and ROS. We found that these treatments led to an improvement in the general condition of the rats, BW, KW, biochemical parameters (including UACR, Scr, and UNAG), tubulointerstitial pathological changes, and the expression levels of various markers of renal tubular injury (including IL-6, TGF- β , VEGF, and TLR4). The beneficial

effects of SKI were similar to those of ROS, a potent insulin sensitizer in the clinic.

EMT is an essential process during the early stages of DKD, not only in the pathogenesis of TIF, but also in the mechanisms that lead to glomerulosclerosis (Loeffler and Wolf, 2015). It is well known that one of the recognized hallmarks of EMT is a clear gain in certain properties of the mesenchymal cells, including the expression of vimentin, α -SMA, and collagen I (Liu, 2004). Our previous study demonstrated that SKI can attenuate fibrotic tubulointerstitial damage in a rat model of unilateral ureteral obstruction (UUO) by blocking pericyte-myofibroblast transition, a process that is known to be similar to EMT (Liu et al., 2019). In this study, we examined a range of EMT markers (including vimentin, α -SMA, and collagen I) in diabetic kidneys to investigate whether SKI and ROS can alleviate renal tubular EMT. Our results revealed that the immunostaining of collagen I and vimentin in the renal tubular epithelial cells, and increased protein expression levels of collagen I, vimentin, and α -SMA, in the kidneys of the DKD rats were significantly reduced following

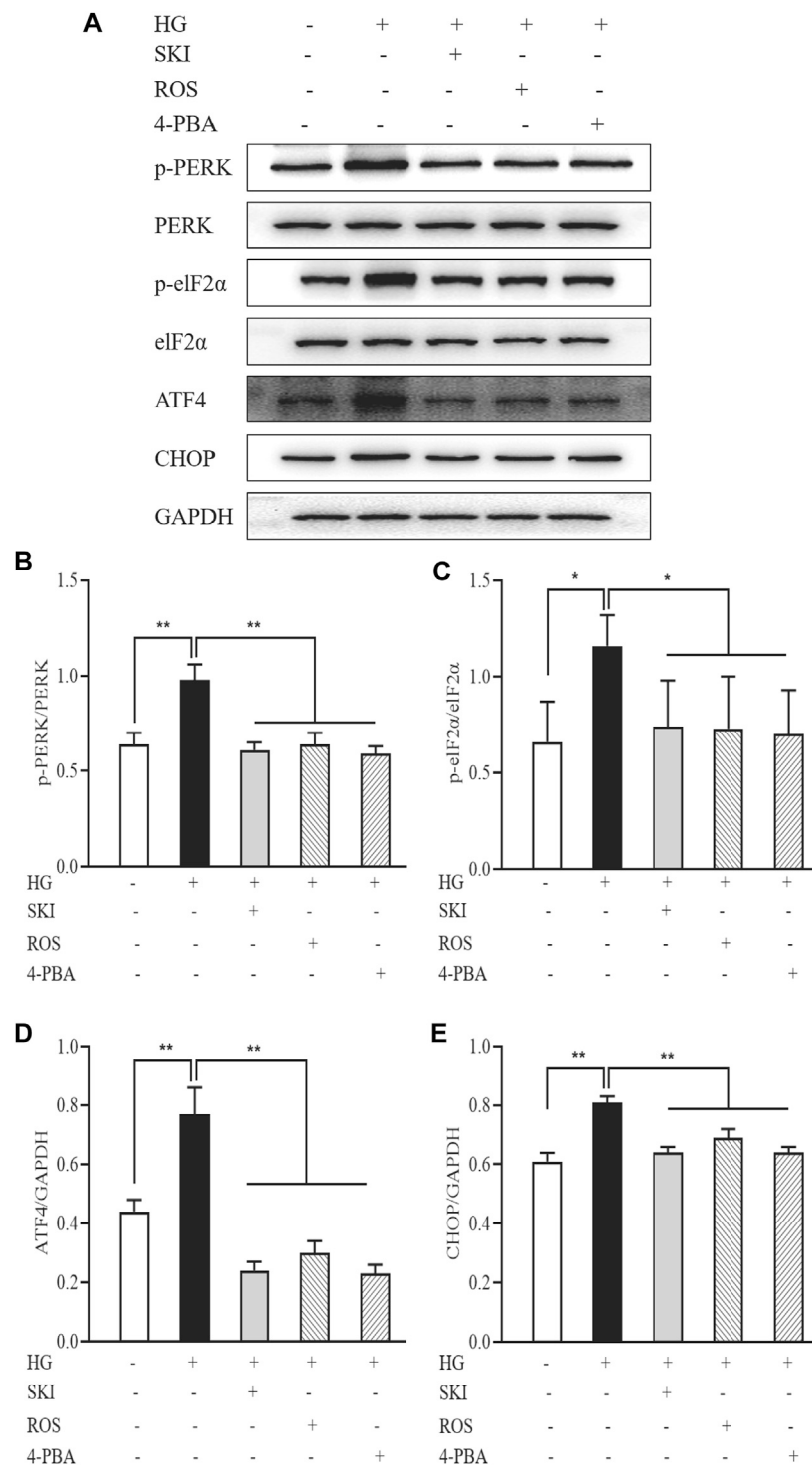
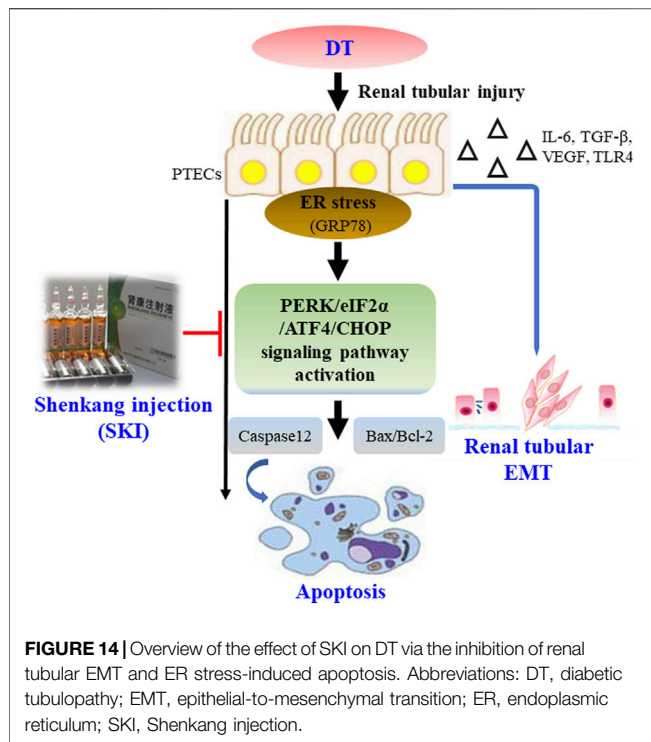


FIGURE 13 | The effects of SKI and ROS on the expression levels of key signaling molecules in the PERK-eIF2 α -ATF4-CHOP pathway *in vitro*. **(A)** WB analysis of p-PERK, PERK, p-eIF2 α , eIF2 α , ATF4, and CHOP, in NRK-52E cells exposed to HG and 4-PBA with or without SKI or ROS for 24 h **(B-E)** The rate of p-PERK to PERK and p-eIF2 α to eIF2 α , and the rate of ATF4 and CHOP to GAPDH, respectively. Data are expressed as mean \pm S.E. * $p < 0.05$, ** $p < 0.01$. Abbreviations: PERK, double-stranded RNA (PKR)-activated protein kinase-like eukaryotic translation initiation factor 2 α (eIF2 α) kinase; eIF2 α , double-stranded RNA (PKR)-activated protein kinase-like eukaryotic translation initiation factor 2 α ; ATF4, activating transcription factor 4; CHOP, C/EBP homologous protein; WB, Western blot; GAPDH, glyceraldehyde-3-phosphate dehydrogenase; HG, high glucose; 4-PBA, 4-phenylbutyric acid; ROS, rosiglitazone; SKI, Shenkang injection.



6 weeks of treatment with SKI or ROS. We therefore considered that SKI could significantly attenuate renal tubular EMT in the rat model of DKD in a manner that was similar to ROS.

An accumulating body of evidence, from both clinical scenarios and experimental animal models, supports the fact that hyperglycemia induces apoptosis through ER stress in tubular cells, at least in part, and that this process contributes to the pathogenesis of DT (Kang et al., 2020). ER stress generally occurs under normal physiological and pathological conditions and represents an important inducer of cell apoptosis (Cybulsky, 2017). In the present study, we used TUNEL-positive tubular cells and abnormal expression levels of Bax, Bcl-2, and GRP78, as well established markers of apoptosis and ER stress. Furthermore, caspase12 is exclusively localized in the ER and is ubiquitously and constitutively expressed. However, unlike other caspases, caspase12 is specifically activated by insults that induce ER stress and not by other death stimuli (Cunard, 2015). In the present study, our data indicated that 6 weeks of SKI and ROS treatment led to significant improvements in the number of TUNEL-positive tubular cells, and ameliorated the high protein expression levels of Bax and caspase12, and the reduced protein expression levels of Bcl-2, in the kidneys of DKD rats. In addition, to confirm whether SKI and ROS were able to reduce ER stress-induced apoptosis in renal tubular cells, we tested the protein expression levels of Bax, Bcl-2, and caspase12, in NRK-52E cells exposed to HG with or without SKI or ROS for 24 h. Our data indicated that the increased protein expression levels of Bax, caspase12, and GRP78, and the reduced protein expression levels of Bcl-2, in NRK-52E cells exposed to HG were significantly ameliorated following treatment with SKI or ROS. Consequently,

we considered that both SKI and ROS are able to alleviate ER stress-induced apoptosis, both *in vivo* and *in vitro*.

Previous research demonstrated that activation of the PERK-eIF2 α -ATF4-CHOP signaling pathway is involved in ER stress-induced podocyte apoptosis in diabetic rats, and that astragaloside IV, the main active component of SKI, can inhibit ER stress-induced podocyte apoptosis by suppressing the PERKATF4-CHOP pathway, at least in part (Chen et al., 2014). In addition, Wang et al. reported that activation of PERK-eIF2 α -ATF4-CHOP signaling axis triggered by excessive ER stress leads to apoptosis in the proximal tubular cells of a rat model of nephrotoxicity (Wang et al., 2019). By regulating the activation of the PERK-eIF2 α -ATF4-CHOP signaling pathway, we hypothesized that it might be possible to identify novel therapeutic mechanisms for SKI and ROS in terms of the inhibition of ER stress-induced apoptosis. Our data clearly demonstrated increased protein expression levels of p-PERK, p-eIF2 α , ATF4, and CHOP in the kidneys of DKD rats and in NRK-52E cells exposed to HG. Collectively, these *in vivo* and *in vitro* findings, provided strong evidence to support the fact that the PERK-eIF2 α -ATF4-CHOP signaling pathway is activated in diabetic kidneys and PTECs. Furthermore, our *in vivo* and *in vitro* experiments showed that SKI and ROS both reduced the level of phosphorylation on key signaling molecules within this key pathway, as well as the expression levels of Bcl-2 protein downstream. In addition, we found that 4-PBA (a specific inhibitor of ER stress) exerted significant suppressive effects on the activation of the PERK-eIF2 α -ATF4-CHOP signaling pathway and ER stress-induced apoptosis in PTECs exposed to HG. It was clear that the *in vitro* regulatory effects of SKI on the activation of the PERK-eIF2 α -ATF4-CHOP signaling pathway were similar to those evoked by a specific ER stress inhibitor. We therefore considered that SKI and ROS could suppress the activation of the PERK-eIF2 α -ATF4-CHOP signaling pathway, both *in vivo* and *in vitro*.

Finally, it is important that we discuss four additional points. First, we chose 5 g/kg/day as a dose for SKI because our previous studies showed that this particular dose of SKI not only attenuated tubulointerstitial damage in the rat model of UUO model but also had no negative effects on liver function (Liu et al., 2019). Second, why we used ROS as a control in this study? Several reports show the effects of thiazolidinediones (TZDs) including ROS on ER stress. It is well known that ER stress is involved in the development of insulin resistance and type 2 diabetes mellitus, and TZDs are antidiabetic agents that act as a potent insulin sensitizer (Kang et al., 2013; Kang et al., 2020). Thus, targeting ER stress in diabetic kidneys, ROS was chosen as a positive control in this study. Third, it is important that we identify the specific targets of SKI that possess the ability to alleviate DT. Although SKI inhibited the activation of the PERK-eIF2 α -ATF4-CHOP signaling pathway *in vivo* and *in vitro*, in a similar manner as 4-PBA (a specific inhibitor of ER stress), we are unable to identify the specific molecules involved in this signaling pathway. Future research should aim to identify the therapeutic targets of SKI and therefore demonstrate how the PERK-eIF2 α -ATF4-CHOP signaling pathway can regulate ER stress-induced apoptosis.

CONCLUSION

This study demonstrated that SKI can alleviate DT by inhibiting EMT and ER stress-induced apoptosis, both *in vivo* and *in vitro* (Figure 14); the actions of SKI were similar to those of ROS. Our findings provide novel information relating to the potential clinical value of SKI in the treatment of DT.

DATA AVAILABILITY STATEMENT

The original contributions presented in the study are included in the article/Supplementary Material, further inquiries can be directed to the corresponding authors.

ETHICS STATEMENT

The animal study was reviewed and approved by the Animal Ethics Committee of Nanjing University Medical School. Written informed consent was obtained from the owners for the participation of their animals in this study.

AUTHOR CONTRIBUTIONS

Y-GW and WW conceived and designed this research. W-WW, Y-LL, M-ZW, HL, B-HL, YT, C-CY, Q-JF, J-XC, JW, and YF performed the experiments. W-WW, Y-LL, M-ZW, and Z-YW analyzed and interpreted the data. W-WW, Y-LL, and M-ZW prepared the figures. W-WW, Y-LL, and M-ZW drafted the manuscript. Y-GW and WW edited and revised the manuscript. W-WW, Y-LL, M-ZW, and YGW approved the final version of the manuscript and all authors approved the final edited version.

FUNDING

This research was supported by the National Natural Science Foundation of China (Grant Nos: 81573903 and 81603675), the

REFERENCES

- Alicic, R. Z., Rooney, M. T., and Tuttle, K. R. (2017). Diabetic Kidney Disease. *Cjasn* 12, 2032–2045. doi:10.2215/CJN.11491116
- Chen, C., Wang, C., Hu, C., Han, Y., Zhao, L., Zhu, X., et al. (2017). Normoalbuminuric Diabetic Kidney Disease. *Front. Med.* 11, 310–318. doi:10.1007/s11684-017-0542-7
- Chen, Y., Gui, D., Chen, J., He, D., Luo, Y., and Wang, N. (2014). Down-regulation of PERK-ATF4-CHOP Pathway by Astragaloside IV Is Associated with the Inhibition of Endoplasmic Reticulum Stress-Induced Podocyte Apoptosis in Diabetic Rats. *Cell Physiol. Biochem.* 33, 1975–1987. doi:10.1159/000362974
- Cunard, R. (2015). Endoplasmic Reticulum Stress in the Diabetic Kidney, the Good, the Bad and the Ugly. *Jcm* 4, 715–740. doi:10.3390/jcm4040715
- Cybulsky, A. V. (2017). Endoplasmic Reticulum Stress, the Unfolded Protein Response and Autophagy in Kidney Diseases. *Nat. Rev. Nephrol.* 13, 681–696. doi:10.1038/nrneph.2017.129

Fundamental Research Funds for the Central Universities (Grant No: 021414380518), the Natural Science Foundation of Jiangsu Province for Young Scholars (Grant No: BK20161046), the Traditional Chinese Medicine Science and Technology Development Program of Jiangsu Province (Grant No: YB201937), Jiangsu Provincial Scientific Research Innovation Fund for post-secondary graduate students (Grant No: KYCX21_1699, KYCX21_1712, KYCX20_1546, SJCX21_0672), the Nanjing Medical Science and Technology Development Project (Grant number: YKK20085), and the Nanjing Famous TCM Doctor's Studio Programme (Grant number: No).

ACKNOWLEDGMENTS

The authors thank Professor Jian Yao (Division of Molecular Signaling, Department of Advanced Biomedical Research, Interdisciplinary Graduate School of Medicine and Engineering, University of Yamanashi, Yamanashi, Japan) and Wei Hu (Department of Pharmacy, Nanjing Drum Tower Hospital, The Affiliated Hospital of Nanjing University Medical School, Nanjing, China) for their helpful discussions and technical assistance.

SUPPLEMENTARY MATERIAL

The Supplementary Material for this article can be found online at: <https://www.frontiersin.org/articles/10.3389/fphar.2021.662706/full#supplementary-material>

Supplementary Figure S1 | Fingerprint analysis of SKI by HPLC. (A) Chromatograms produced from mixed standards, (B) SKI samples. Abbreviations: SKI, Shengkang injection; HPLC, high performance liquid chromatography.

Supplementary Figure S2 | Animal experimental protocols.

Supplementary Figure S3 | Cell viability in cultured NRK-52E cells. (A) Cultured NRK-52E cells were exposed to HG with SKI at 10, 20, and 40 µg/ml for 24 h; (B) Cultured NRK-52E cells were exposed to HG with ROS at 50, 100, and 200 nmol/L for 24 h. Abbreviations: HG, high glucose; ROS, rosiglitazone; SKI, Shengkang injection.

- Gilbert, R. E., and Cooper, M. E. (1999). The Tubulointerstitium in Progressive Diabetic Kidney Disease: More Than an Aftermath of Glomerular Injury?. *Kidney Int.* 56, 1627–1637. doi:10.1046/j.1523-1755.1999.00721.x
- Han, W., Ma, Q., Liu, Y., Wu, W., Tu, Y., Huang, L., et al. (2019). Huangkui Capsule Alleviates Renal Tubular Epithelial-Mesenchymal Transition in Diabetic Nephropathy via Inhibiting NLRP3 Inflammasome Activation and TLR4/NF-κB Signaling. *Phytomedicine* 57, 203–214. doi:10.1016/j.phymed.2018.12.021
- Kang, J. M., Lee, H.-S., Kim, J., Yang, D. H., Jeong, H. Y., Lee, Y. H., et al. (2020). Beneficial Effect of Chloroquine and Amodiaquine on Type 1 Diabetic Tubulopathy by Attenuating Mitochondrial Nox4 and Endoplasmic Reticulum Stress. *J. Korean Med. Sci.* 35, e305. doi:10.3346/jkms.2020.35.e305
- Kang, M.-K., Park, S.-H., Kim, Y.-H., Lee, E.-J., Antika, L. D., Kim, D. Y., et al. (2017). Chrysin Ameliorates Podocyte Injury and Slit Diaphragm Protein Loss via Inhibition of the PERK-eIF2α-ATF-CHOP Pathway in Diabetic Mice. *Acta Pharmacol. Sin.* 38, 1129–1140. doi:10.1038/aps.2017.30
- Kang, S. B., Kim, H. M., Kim, H. J., Seok, H., Huh, J. H., Lee, B.-W., et al. (2013). Rosiglitazone Attenuates Casein-Induced Hepatic Endoplasmic Reticulum

- Stress in Sprague-Dawley Rats: a Novel Model of Endoplasmic Reticulum Stress. *Endocr. J.* 60, 1231–1240. doi:10.1507/endocrj.ej13-0167
- Kitamura, M. (2008a). Endoplasmic Reticulum Stress and Unfolded Protein Response in Renal Pathophysiology: Janus Faces. *Am. J. Physiology-Renal Physiol.* 295, F323–F334. doi:10.1152/ajprenal.00050.2008
- Kitamura, M. (2009). Endoplasmic Reticulum Stress in Glomerulonephritis: the Bad Guy Turns Good?. *Jasn* 20, 1871–1873. doi:10.1681/ASN.2009060581
- Kitamura, M. (2008b). Endoplasmic Reticulum Stress in the Kidney. *Clin. Exp. Nephrol.* 12, 317–325. doi:10.1007/s10157-008-0060-7
- Lee, Y. H., Kim, S. H., Kang, J. M., Heo, J. H., Kim, D.-J., Park, S. H., et al. (2019). Empagliflozin Attenuates Diabetic Tubulopathy by Improving Mitochondrial Fragmentation and Autophagy. *Am. J. Physiology-Renal Physiol.* 317, F767–F780. doi:10.1152/ajprenal.00565.2018
- Liu, B.-H., Chong, F.-L., Yuan, C.-C., Liu, Y.-L., Yang, H.-M., Wang, W.-W., et al. (2021). Fucoidan Ameliorates Renal Injury-Related Calcium-Phosphorus Metabolic Disorder and Bone Abnormality in the CKD-MBD Model Rats by Targeting FGF23-Klotho Signaling Axis. *Front. Pharmacol.* 11, 586725. doi:10.3389/fphar.2020.586725
- Liu, B., Tu, Y., He, W., Liu, Y., Wu, W., Fang, Q., et al. (2018). Hyperoside Attenuates Renal Aging and Injury Induced by D-Galactose via Inhibiting AMPK-ULK1 Signaling-Mediated Autophagy. *Aging* 10, 4197–4212. doi:10.18632/aging.101723
- Liu, Y., Shi, G., Yee, H., Wang, W., Han, W., Liu, B., et al. (2019). ShenKang Injection, a Modern Preparation of Chinese Patent Medicine, Diminishes Tubulointerstitial Fibrosis in Obstructive Nephropathy via Targeting Pericyte-Myofibroblast Transition. *Am. J. Transl. Res.* 11, 1980–1996. PMID: 31105812.
- Liu, Y. (2004). Epithelial to Mesenchymal Transition in Renal Fibrogenesis: Pathologic Significance, Molecular Mechanism, and Therapeutic Intervention. *J. Am. Soc. Nephrol.* 15, 1–12. doi:10.1097/01.asn.0000106015.29070.e7
- Loeffler, I., and Wolf, G. (2015). Epithelial-to-mesenchymal Transition in Diabetic Nephropathy: Fact or Fiction?. *Cells* 4, 631–652. doi:10.3390/cells4040631
- Ma, R. C. W. (2018). Epidemiology of Diabetes and Diabetic Complications in China. *Diabetologia* 61, 1249–1260. doi:10.1007/s00125-018-4557-7
- Mao, Z.-M., Shen, S.-M., Wan, Y.-G., Sun, W., Chen, H.-L., Huang, M.-M., et al. (2015). Huangkui Capsule Attenuates Renal Fibrosis in Diabetic Nephropathy Rats through Regulating Oxidative Stress and p38MAPK/Akt Pathways, Compared to α -lipoic Acid. *J. Ethnopharmacology* 173, 256–265. doi:10.1016/j.jep.2015.07.036
- Min, S.-Y., Ha, D.-S., and Ha, T.-S. (2018). Puromycin Aminonucleoside Triggers Apoptosis in Podocytes by Inducing Endoplasmic Reticulum Stress. *Kidney Res. Clin. Pract.* 37, 210–221. doi:10.23876/j.krcp.2018.37.3.210
- Oakes, S. A. (2020). Endoplasmic Reticulum Stress Signaling in Cancer Cells. *Am. J. Pathol.* 190, 934–946. doi:10.1016/j.ajpath.2020.01.010
- Oakes, S. A., and Papa, F. R. (2015). The Role of Endoplasmic Reticulum Stress in Human Pathology. *Annu. Rev. Pathol. Mech. Dis.* 10, 173–194. doi:10.1146/annurev-pathol-012513-104649
- Song, Z., Qin, T., Pan, Y., Wu, L., Liu, T., and Hua, Q. (2019). ShenKang Injection Improves Coagulation in Patients with Chronic Kidney Disease: a Systematic Review and Meta-Analysis. *J. Tradit. Chin. Med.* 39, 451–458. PMID: 32186091.
- Tang, S. C. W., Chan, L. Y. Y., Leung, J. C. K., Cheng, A. S., Chan, K. W., Lan, H. Y., et al. (2010). Bradykinin and High Glucose Promote Renal Tubular Inflammation. *Nephrol. Dial. Transplant.* 25, 698–710. doi:10.1093/ndt/gfp599
- Tang, S. C. W., Leung, J. C. K., and Lai, K. N. (2011). Diabetic Tubulopathy: an Emerging Entity. *Contrib. Nephrol.* 170, 124–134. doi:10.1159/000325647
- Tu, Y., Fang, Q.-J., Sun, W., Liu, B.-H., Liu, Y.-L., Wu, W., et al. (2020). Total Flavones of *Abelmoschus Manihot* Remodels Gut Microbiota and Inhibits Microinflammation in Chronic Renal Failure Progression by Targeting Autophagy-Mediated Macrophage Polarization. *Front. Pharmacol.* 11, 566611. doi:10.3389/fphar.2020.566611
- Umanath, K., and Lewis, J. B. (2018). Update on Diabetic Nephropathy: Core Curriculum 2018. *Am. J. Kidney Dis.* 71, 884–895. doi:10.1053/j.ajkd.2017.10.026
- Vallon, V. (2011). The Proximal Tubule in the Pathophysiology of the Diabetic Kidney. *Am. J. Physiology-Regulatory, Integr. Comp. Physiol.* 300, R1009–R1022. doi:10.1152/ajpregu.00809.2010
- Wang, M.-G., Fan, R.-F., Li, W.-H., Zhang, D., Yang, D.-B., Wang, Z.-Y., et al. (2019). Activation of PERK-eIF2 α -ATF4-CHOP axis Triggered by Excessive ER Stress Contributes to lead-induced Nephrotoxicity. *Biochim. Biophys. Acta (Bba) - Mol. Cel Res.* 1866, 713–726. doi:10.1016/j.bbamcr.2018.12.002
- Wu, W., Hu, W., Han, W.-B., Liu, Y.-L., Tu, Y., Yang, H.-M., et al. (2018). Inhibition of Akt/mTOR/p70S6K Signaling Activity with Huangkui Capsule Alleviates the Early Glomerular Pathological Changes in Diabetic Nephropathy. *Front. Pharmacol.* 9, 443. doi:10.3389/fphar.2018.00443
- Wu, W., Yang, J.-J., Yang, H.-M., Huang, M.-M., Fang, Q.-J., Shi, G., et al. (2017). Multi-glycoside of Tripterygium Wilfordii Hook. F. Attenuates Glomerulosclerosis in a Rat Model of Diabetic Nephropathy by Exerting Anti-microinflammatory Effects without Affecting Hyperglycemia. *Int. J. Mol. Med.* 40, 721–730. doi:10.3892/ijmm.2017.3068
- Xu, S., Lv, Y., Zhao, J., Wang, J., Zhao, X., and Wang, S. (2016). Inhibitory Effects of ShenKang Injection and its Main Component Emodin on the Proliferation of High Glucose-Induced Renal Mesangial Cells through Cell Cycle Regulation and Induction of Apoptosis. *Mol. Med. Rep.* 14, 3381–3388. doi:10.3892/mmr.2016.5631
- Xu, T., Zuo, L., Sun, Z., Wang, P., Zhou, L., Lv, X., et al. (2017). Chemical Profiling and Quantification of ShenKang Injection, a Systematic Quality Control Strategy Using Ultra High Performance Liquid Chromatography with Q Exactive Hybrid Quadrupole Orbitrap High-Resolution Accurate Mass Spectrometry. *J. Sep. Sci.* 40, 4872–4879. doi:10.1002/jssc.201700928
- Yao, S., Zhang, J., Wang, D., Hou, J., Yang, W., Da, J., et al. (2015). Discriminatory Components Retracing Strategy for Monitoring the Preparation Procedure of Chinese Patent Medicines by Fingerprint and Chemometric Analysis. *PLoS One* 10, e0121366. doi:10.1371/journal.pone.0121366
- Zeni, L., Norden, A. G. W., Cancarini, G., and Unwin, R. J. (2017). A More Tubulocentric View of Diabetic Kidney Disease. *J. Nephrol.* 30, 701–717. doi:10.1007/s40620-017-0423-9
- Zou, J.-J., Zhou, X.-T., Chen, Y.-K., Liu, J.-L., Wang, C., Ma, Y.-R., et al. (2020). A Review on the Efficacy and Mechanism of Action of ShenKang Injection against Chronic Kidney Disease. *Biomed. Pharmacother.* 132, 110833. doi:10.1016/j.biopha.2020.110833

Conflict of Interest: The authors declare that the research was conducted in the absence of any commercial or financial relationships that could be construed as a potential conflict of interest.

Publisher's Note: All claims expressed in this article are solely those of the authors and do not necessarily represent those of their affiliated organizations, or those of the publisher, the editors and the reviewers. Any product that may be evaluated in this article, or claim that may be made by its manufacturer, is not guaranteed or endorsed by the publisher.

Copyright © 2021 Wang, Liu, Wang, Li, Liu, Tu, Yuan, Fang, Chen, Wang, Fu, Wan, Wan and Wu. This is an open-access article distributed under the terms of the Creative Commons Attribution License (CC BY). The use, distribution or reproduction in other forums is permitted, provided the original author(s) and the copyright owner(s) are credited and that the original publication in this journal is cited, in accordance with accepted academic practice. No use, distribution or reproduction is permitted which does not comply with these terms.

GLOSSARY

- Alb** serum albumin
- ATF4** activating transcription factor 4
- BG** blood glucose
- BUN** blood urea nitrogen
- BW** body weight
- collagen I** collagen type I
- CHOP** C/EBP homologous protein
- DKD** diabetic kidney disease
- DM** diabetes mellitus;
- DT** diabetic tubulopathy
- eIF2 α** double-stranded RNA (PKR)-activated protein kinase-like eukaryotic translation initiation factor 2 α
- ECM** extracellular matrix
- EMT** epithelial-to-mesenchymal transition
- ER** endoplasmic reticulum
- GAPDH** glyceraldehyde-3-phosphate dehydrogenase
- GRP78** glucose-regulated protein 78
- HPLC** high performance liquid chromatography
- HG** high glucose
- IHC** immunohistochemistry;
- IL-6** interleukin-6
- KW** kidney weight
- LSD** least significant difference
- PAS** Periodic acid-Schiff
- PERK** double-stranded RNA (PKR)-activated protein kinase-like eukaryotic translation initiation factor 2 α (eIF2 α) kinase
- PTECs** proximal tubular epithelial cells
- ROS** rosiglitazone;
- SKI** Shenkang injection
- Scr** serum creatinine
- SDS** sodium dodecyl sulfate
- STZ** streptozocin
- TGF- β** transforming growth factor- β
- TLR4** toll-like receptor 4
- TUNEL** terminal deoxynucleotidyl transferase dUTP nick end labeling
- UACR** urinary microalbumin to creatinine
- UNAG** urinary *N*-acetyl-beta-*D*-glucosaminidase
- VEGF** vascular endothelial growth factor
- WB** Western blot
- α -SMA** α -smooth muscle actin
- 4-PBA** 4-phenylbutyric acid.